SCIENCE CHINA
Physics, Mechanics & Astronomy

•Article•

February 2021 Vol. 64 No. 2: 224611
https://doi.org/10.1007/s11433-020-1614-5

Grain boundary segregation and relaxation in nano-grained polycrystalline alloys

Tong-Yi Zhang*, Ying-Xin Gao, and Sheng Sun*

Materials Genome Institute, Shanghai University, Shanghai 200444, China

Received July 30, 2020; accepted August 18, 2020; published online December 30, 2020

The present study carries out systematic thermodynamics analysis of Grain Boundary (GB) segregation and relaxation in Nano-Grained (NG) polycrystalline alloys. GB segregation and relaxation is an internal process towards thermodynamic equilibrium, which occurs naturally in NG alloys without any applied loads, causes deformation and generates internal stresses. The analysis comprehensively investigates the multiple coupling effects among chemical concentrations and mechanical stresses in GBs and grains. A hybrid approach of eigenstress and eigenstrain is developed herein to solve the multiple coupling problem. The analysis results indicate that the GB stress and grain stress induced by GB segregation and relaxation can be extremely high in NG alloys, reaching the GPa level, which play an important role in the thermal stability of NG alloys, especially via the coupling terms between stress and concentration. The present theoretic analysis proposes a novel criterion of thermal stability for NG alloys, which is determined by the difference in molar free energy between a NG alloy and its reference single crystal with the same nominal chemical composition. If the difference at a temperature is negative or zero, the NG alloy is thermal stable at that temperature, otherwise unstable.

nano-grained alloys, thermal stability, grain boundary segregation, eigenstress, eigenstrain

PACS number(s): 62.25.-g, 64.75.Jk, 68.35.Gy

Citation: T.-Y. Zhang, Y.-X. Gao, and S. Sun, Grain boundary segregation and relaxation in nano-grained polycrystalline alloys, Sci. China-Phys. Mech. Astron. **64**, 224611 (2021), https://doi.org/10.1007/s11433-020-1614-5

1 Introduction

Reducing grain size is the most efficient approach to improve the mechanical properties of metals and alloys, as indicated by the Hall-Petch equation [1,2]. When the grain size of a material is smaller than 100 nm, the material is called Nano-Grained (NG) material. In addition to the improved mechanical properties, NG materials possess unique thermodynamic properties, which distinguish them from their Coarse-Grained (CG) (or single crystalline) counterparts and make their properties size dependent [3-6]. A large amount of Grain Boundaries (GBs) in a NG material implies high total GB energy, which is the driving force for grain growth. That is why NG materials could be thermodynamically unstable and grain growth could happen, especially at elevated temperature. Grain growth is usually significant in pure NG metals of mono-element and occurs at relatively low temperature [7]. In the literature, two approaches are reported to stabilize nanograins. The first approach against grain coarsening is appropriate alloying that brings GB segregation and hence lowers the total GB energy. For example, Chookajorn et al. [8] proposed a nanostructure stability map, based on a thermodynamic model, for the design of thermal stable NG alloys. They verified this approach with NG W-Ti alloys and demonstrated substantially enhanced stability for the high-

*Corresponding authors (Tong-Yi Zhang, email: zhangty@shu.edu.cn; Sheng Sun, email: mgissh@t.shu.edu.cn)

temperature, long-duration conditions amenable to powder-route production of bulk nanostructured tungsten. Hu et al. [9] experimentally investigated the GB stability and the hardening and softening behaviors in NG Ni-Mo alloys with the nominal Mo concentration ranging from 0 to 21.5 at%. Their results indicate that the onset temperature for grain coarsening with annealing duration of 1 h increases with the increase in nominal Mo concentration because more Mo atoms move to and segregate in GBs, which gives the Ni-Mo NG alloys ultrahigh hardness. Although segregation occurs on twin boundaries [10] and phase boundaries [6], the present work focuses on normal GBs, rather than twin boundaries and phase boundaries. The other approach to prevent NG metals from grain coarsening is to render GBs low energy, as illustrated by Zhou et al. [11] in pure Cu and Ni. They experimentally discovered that NG pure Cu and Ni metals produced from cold working exhibited notable thermal stability below a critical grain size, beyond which the smaller the grain size was, the higher the instability temperature would be. The inherent thermal stability of nanograins was originated from an autonomous GB evolution to low-energy states due to the activation of partial dislocations in cold working. Zhou et al. [12] further investigated the size dependence of GB migration in NG metals of pure Ag, Cu, and Ni, and found that as grain size decreased, GB migration intensified and then diminished below a critical grain size, which was attributed to low GB energy state via relaxation. The present work studies the GB segregation and relaxation simultaneously and re-explores the thermodynamic framework for the design of thermal stable NG alloys. This is because that thermodynamic energy analysis is essential and fundamental in the development of thermal stability criteria for NG materials, although kinetics describes and determines the microstructure evolution.

There are a lot of publications in the literature on the thermodynamic study of NG material stabilization. For example, Weissmüller [13] conducted thermodynamic analysis for NG alloys by following Cahn's layer treatment of GBs [14]. Fecht [15] proposed a simple method to describe the thermodynamic properties of disordered GBs in NG metals and semiconductors. Based on a universal equation of state [16] and the Grüneisen parameter [17], Fecht [15] derived the maximum free volume, thermal expansion coefficient, specific-heat capacity, excess enthalpy, excess entropy, and excess free energy of GBs and his results showed good agreement with available experimental data. Kalidindi et al. [18] provided a thermodynamics review on NG material stabilization by alloying with the emphasizing on Monte Carlo simulations, where a NG state was considered to be stable if the NG alloy had the lowest free energy available to the alloy system, such that it was stable against both grain growth and the formation of bulk second phase. By comparing the enthalpy of the GB segregated state against such stable bulk phases, Kalidindi and Schuh [19] proposed a stability criterion for NG alloys. With this criterion, their Monte Carlo simulations showed that entropy could play a role in stabilizing NG alloys. Besides, phase field simulations [20] have been conducted to investigate GB segregation in immiscible NG alloys. Dingreville and Berbenni [21] analyzed the interaction of solutes with GBs by using disclination model. Zhang and Hack [22] used three-dimensional (3D) interphase treatment to study the effect of GBs on the elastic properties of NG materials. Lejček and Hofmann [23] proposed three parameters to estimate GB segregation, which were the standard enthalpy of GB segregation, the standard entropy of GB segregation, and the Fowler binary interaction coefficient, and then applied the model to iron-based binary systems. Peng et al. [24] reviewed the progress in the research on the thermal stability of NG materials and concluded that the reduction of GB energy by solute segregation was an effective approach of thermodynamic and kinetic stabilization of NG alloys, which enhanced the thermal stability of grain size against coarsening at elevated temperatures. Saber et al. [25] provided an overview on thermodynamic grain size stabilization models proposed by Weissmüller [13,26], Kirchheim et al. [27-29], Darling et al. [30], Trelewicz and Schuh [31], Saber et al. [32,33]. The overview discussed application windows of each stabilization model. They preferred the TS model [31], which could be applied to thermodynamic stabilization of non-dilute systems with either weakly or strongly segregating solutes. They also pointed out that the role of elastic enthalpy due to the atomic size misfit was not considered in the TS model. Wynblatt and Ku [34] approximately treated the total enthalpy of segregation as the linear combination of the elastic and chemical enthalpies of segregation. The elastic enthalpy of segregation is the released strain energy when solute atoms move to and segregate in GBs from lattice, while the chemical enthalpy of segregation counts for the chemical (bond energy) contribution. By using the linear combination of the elastic and chemical enthalpies of segregation [34] and the released elastic strain energy [35], Saber et al. [32,33] modified the TS model and enhanced the prediction power of the thermodynamic grain stabilization model. Tang et al. [36] developed a model, combining first principles calculations and thermodynamics, to study the thermal stability of NG alloys. Krauß and Eich [37] proposed an equivalent single layer with identical segregation properties to account for all subsurface layer effects and Zhang et al. [38] employed the similar approach to calculate the surface energy density after relaxation. Voorhees and Johnson [39] overviewed the thermodynamics of elastically stressed crystals. Nevertheless, the role of stress in the thermodynamic stability of NG alloys has not been systematically studied so far due to the challenge that internal stresses in GBs and grains are nonlinearly coupled with chemical con-

centrations in GBs and grains, as illustrated in the previous work [40]. The goal of the present study is to investigate the multiple coupling behaviors of chemical compositions and internal stresses in GB segregation and relaxation, and in thermal stability of NG alloys by systematically thermodynamic analysis.

Figure 1 schematically shows the multiple interactions between stresses and concentrations in grain lattice and GBs of a NG polycrystalline alloy at a given temperature without any external loads. The left part of Figure 1 indicates the stress interaction between grain lattice and GBs, where a grain exerts stress on its GBs and the GBs apply stress on the grain. Since these stresses are internal, the resultant force acting on the entire system of a grain and its GBs must be zero, meaning that the generalized capillary equation of force balance [41-43] links GB stress and grain stress. The right part of Figure 1 shows the interaction of concentration between the grain and its GBs, illustrating GB segregation. Based on the 3D interphase treatment of GBs, the Gibbs adsorption isotherm [44] and the McLean adsorption isotherm [45], Zhang and Ren [40] developed a Gibbs-approach-based adsorption isotherm (or generalized McLean adsorption isotherm called herein) for GB segregation in NG polycrystals, which is used in the present work and will be described in detail in the following theoretical analysis. The top part of Figure 1 illustrates the coupling between stress and concentration. On top right side, the difference in concentration generates a strain field and then a stress field, which can be calculated from the eigenstrain approach. Eigenstrain and eigenstress denote stress-free strain and strain-free stress, respectively. Eigenstrain describes the degree of deformation induced by other physical/chemical fields, rather than mechanical stress, while eigenstress characterizes the change in stress induced by other physical/chemical fields, rather than mechanical deformation. Eigenstrain and eigenstress approaches are widely employed in micro/nanomechanics [46]. On the top left side, the change in stress causes the redistribution of concentration via stress induced diffusion. At thermodynamic equilibrium, stresses and concentrations in the grain lattice and GBs should reach their equilibrium values, respectively. In the previous work, Zhang and Ren [40] studied the multiple nonlinear coupling behaviors for closed and open systems and later applied the theoretical results to H–Pd solid solutions [47]. Using the experimental data of lattice strain and sample strain of the NG Pd, with an average grain size of 10 nm, versus H_2 partial pressure [48], Ren et al. [47] determined H concentrations and stresses in both grains and GBs, and the GB intrinsic properties. Then, the generalized McLean adsorption isotherm with the determined intrinsic properties has the power to quantitatively predict the size dependent solubility of H in NG Pd with an average grain size of 5 nm. The theoretical prediction agrees with other reported experimental data [49], thereby illustrating the success of the generalized McLean adsorption isotherm. The generalized McLean adsorption isotherm was further developed for nanoparticles [40,50] and nanometer thick films [51]. The present work adopts the generalized McLean adsorption isotherm to thermodynamically analyze the GB segregation and relaxation, and thermal stability of NG materials.

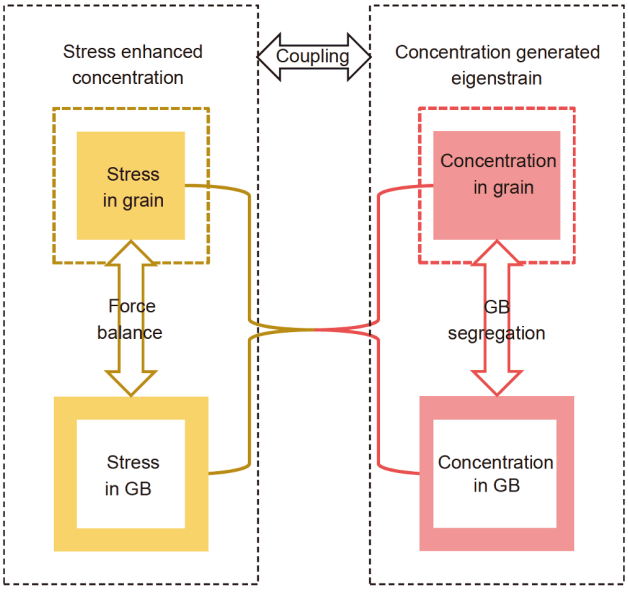

Figure 1 (Color online) Schematic illustration of the interactions between stress and concentration, and between grain lattice and GBs in a NG polycrystalline alloy at a given temperature without any external loads.

2 Theoretical analysis

Following the previous 3D interphase treatment of GBs without considering the atomic arrangement in GBs [40], we analyze the thermodynamic properties of GBs. A polycrystalline alloy is modelled to be a composite of uniformly distributed cubic grains and associated GBs in the present study. Only grains and GBs, GB eigenstress, and GB segregation and relaxation are considered here and other defects and residual stresses are not analyzed for simplicity. Theoretically, a NG alloy with nominal chemical composition can be regarded to be formed from a stress-free bulk single crystalline counterpart, which serves as a reference state in the present thermodynamic analysis. Figure 2(a) is a two-dimensional (2D) drawing, schematically showing the formation process of the NG material. Many nanograins with different orientations are taken out from their single crystal parent and then group together to form a NG alloy. Once a NG alloy is formed with nanograins, GBs appear with excess energy and GB eigenstress, and then GB segregation and relaxation will occur inevitably and naturally to reduce the energy of the NG alloy, which is an internal process within

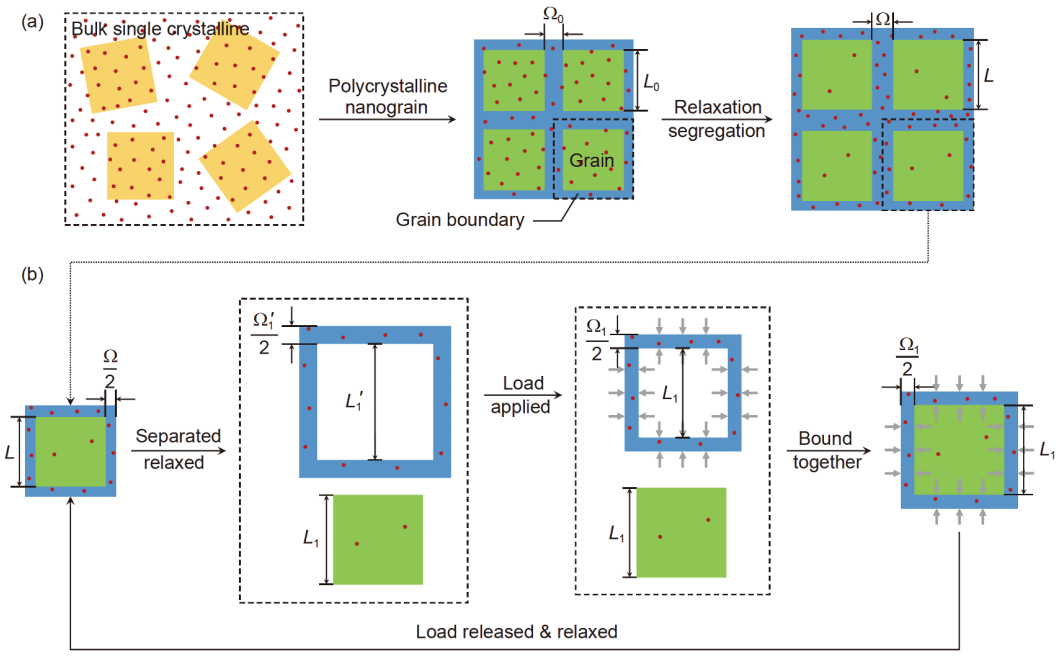

Figure 2 (Color online) (a) Schematic illustration of the formation and GB segregation and relaxation, and (b) schematic illustration of the hybrid approach considering the GB born eigenstress and the segregation induced eigenstrain.

the NG alloy [52]. In the present study, a representative domain is selected in the analysis, which contains a cubic grain and associated GBs. The total volume of a grain and its associated GBs is given by

$$V = V_{\mathrm{g}} + V_{\mathrm{gb}} = (L + \Omega)^3, \tag{1a}$$

where V, L, and Ω denote volume, grain size (the cubic edge length) and GB thickness, respectively, subscripts "g" and "gb" denote grain and GB, respectively. Define the volume fraction of grain by $f_{V,\mathrm{g}} = \frac{V_{\mathrm{g}}}{V}$ and the volume fraction of GBs by $f_{V,\mathrm{gb}} = \frac{V_{\mathrm{gb}}}{V}$. The ratio of GB volume over grain volume is given by

$$f_{V_{\mathrm{gb}}/V_{\mathrm{g}}} = \frac{V_{\mathrm{gb}}}{V_{\mathrm{g}}} = \frac{3\Omega}{L} + \frac{3\Omega^2}{L^2} + \frac{\Omega^3}{L^3} \approx \frac{3\Omega}{L}. \tag{1b}$$

Eq. (1a) holds for NG alloy samples, although the analysis is based on a grain and associated GBs. For polycrystal samples with the same volume, the GB volume (grain volume) will increase (decrease) with the reduction in grain size.

Before GB segregation and relaxation, the chemical composition in the grains and GBs remains unchanged as that in the bulk single crystalline counterpart. During GB segregation and relaxation in such a closed system at a given temperature without any external loads, solute atoms move from grains to GBs and segregate there and some solvent atoms may also move from GBs to grains by exchanging with solute atoms, thereby changing the chemical compositions in GBs and grains. Spontaneous GB segregation and relaxation cause deformation in grains and GBs, and generate internal stresses, although no external mechanical loads and constraints are applied on the NG alloy. The deformation of grains in a NG material is constrained by the associated GBs and vice versa. The free energy F is usually used for such internal process in a closed thermodynamic system at a constant temperature and without any external loads. For the representative system of a grain and its associated 3D interphase GBs, F is the sum of the free energies of the grain and GBs:

$$F = F_{\mathrm{g}} + \widehat{F}_{\mathrm{gb}}, \tag{2a}$$

$$\widehat{F}_{\mathrm{gb}} = F_{\mathrm{gb}} + \Gamma, \tag{2b}$$

where F_g is the free energy of the grain, $\widehat{F}_{\mathrm{gb}}$ is the total GB free energy of the 3D GBs including the free energy of F_{gb} and the total excess free energy of Γ, which is also called the total GB energy. In the Gibbs sharp interface approach, the GB volume nulls and hence F_{gb}=0. The excess free energy density (GB energy density) per unit GB area γ is widely used such that $\Gamma = A\gamma$ with A being the GB area. In the 3D GB approach, the 3D GB energy density per unit volume is introduced and defined by $\hat{\gamma} = \Gamma / V_{\mathrm{gb}} = \Gamma / (A\Omega)$. The 3D GB energy density per unit volume $\hat{\gamma}$ is linked to the 2D GB energy density γ via $\gamma = \hat{\gamma}\,\Omega$. Provided that the GB energy density remains unchanged, the total GB energy, viz. the excess free energy will increase linearly with the GB area. Thus, for NG polycystal samples with the same given mass, the total GB energy usually increases as the grain size gets

small.

The free energy density of a studied system is the sum of three free energy densities, i.e., the chemical energy density, the mechanical energy density, and the gradient energy density [53], which interact to each other, although each of them apparently appears on its own. This approach establishes the thermodynamic foundation of phase field simulations [54]. If without considering the gradient energy, each of the grain and GB free energies is the sum of mechanical energy F^{m} and chemical energy F^{c}, although there is interaction between the mechanical and chemical energies, as illustrated in Figure 1, i.e.,

$$F_{\mathrm{g}} = F_{\mathrm{g}}^{\mathrm{m}} + F_{\mathrm{g}}^{\mathrm{c}}, \tag{2c}$$

$$\widehat{F}_{\mathrm{gb}} = F_{\mathrm{gb}}^{\mathrm{m}} + F_{\mathrm{gb}}^{\mathrm{c}} + \Gamma. \tag{2d}$$

2.1 Mechanical analysis

For simplicity, we consider here only averaged stresses in the grain and GBs, i.e., the averaged hydrostatic stress, σ_{g}, in the grain, the averaged GB in-plane stress, $\sigma_{\mathrm{gb}}^{\parallel}$, along the GB tangential direction, and the averaged GB normal stress, $\sigma_{\mathrm{gb}}^{\perp}$, along the GB perpendicular direction. The surface eigenstress model [55] indicates clearly that a newborn interface is accompanied with interface eigenstress before relaxation. Similarly, GBs are born with GB tangential stress before GB segregation and relaxation, and the born GB tangential stress is called GB eigenstress $\sigma_{\mathrm{gb}}^{\parallel 0}$. When the NG alloy is formed, the internal process of GB segregation and relaxation will occur spontaneously, which lowers the total free energy of the NG alloy and causes deformation and internal stress fields. Usually, the chemical composition related stress analysis is based on the eigenstrain approach, which is in analogy with the thermal stress analysis. On the other hand, the newborn GBs are associated with GB eigenstress. Therefore, the mechanical analysis of GB segregation and relaxation includes eigenstrain and eigenstress and thus a hybrid approach of eigenstrain and eigenstress is developed herein to solve this coupling problem between the segregation induced eigenstrains and the GB born eigenstress. To have analytic solutions, the following simplifications are made in the hybrid approach of eigenstrain and eigenstress: only volumetric deformation is considered for the grain, and biaxial tangential deformation and normal deformation are considered for the GBs; linear elasticity is used without considering any shear deformation; and each of the grain and GBs is treated to be mechanically isotropic. The change in chemical composition induces eigenstrains in the grain and GBs. The differentiation δ of the chemical composition induced eigenstrains is defined by

$$\delta = e_{\mathrm{gb}}^{0} - e_{\mathrm{g}}^{0}, \tag{3a}$$

where e_{g}^{0} and e_{gb}^{0} are the composition change induced eigenstrains in the grain and GBs, respectively, which are called chemical eigenstrains hereafter. The chemical eigenstrains are given by

$$e_{\mathrm{gb}}^{0} = \frac{\sum_{i}^{k} \overline{V}_{\mathrm{gb},i} \Delta n_{\mathrm{gb},i}}{V_{\mathrm{gb0}}}, \tag{3b}$$

$$e_{\mathrm{g}}^{0} = \frac{\sum_{i}^{k} \overline{V}_{\mathrm{g},i} \Delta n_{\mathrm{g},i}}{V_{\mathrm{g0}}}, \tag{3c}$$

where $\overline{V}_{\mathrm{gb},i}$ and $\overline{V}_{\mathrm{g},i}$ are the partial molar volumes of element i in the GBs and grain, respectively, $\Delta n_{\mathrm{gb},i}$ and $\Delta n_{\mathrm{g},i}$ are the changes in mole number of element i in the GBs and grain, respectively, and k is the number of elements. Figure 2(b) schematically shows the mechanical analysis. The grain and the GBs in the thermodynamic equilibrium state are imagined to be isothermally separated with each equilibrium chemical composition and stay at the stress-free state. The grain and the GBs change their sizes at the separated stress-free state, in comparison with the bonded thermodynamic equilibrium state, as shown in Figure 2(b). The size change is caused by the chemical eigenstrains and by the completely release of GB eigenstress. Since the GB eigenstress $\sigma_{\mathrm{gb}}^{\parallel 0}$ is usually tensile, the eigenstrain induced by the release of GB eigenstress will be compressive, whereas the GB segregation induced chemical eigenstrain is also usually tensile. With the separated stress-free state as reference, applying external loads deforms the GBs to fit the size of the stress-free grain. At the perfect fitting state, the GBs are coherently bonded with the stress-free grain, and at this state there are total eigenstresses in the GBs. The chemical eigenstrain differentiation induces the hydrostatic eigenstress $\sigma_{\mathrm{gb}}^{\delta} = -\frac{1}{3} K_{\mathrm{gb}} \delta$ at this state, where K_{gb} is the GB bulk modulus. Thus, the total GB eigenstresses are given by $\sigma_{\mathrm{gb}}^{\parallel 0\delta} = \sigma_{\mathrm{gb}}^{\parallel 0} + \sigma_{\mathrm{gb}}^{\delta}$ and $\sigma_{\mathrm{gb}}^{\perp 0\delta} = \sigma_{\mathrm{gb}}^{\perp \delta} = \sigma_{\mathrm{gb}}^{\delta}$. Consequently, the eigenstress approach is used in mechanical analysis with the total GB eigenstresses. The studied representative nanograin and GBs will relax to reach the thermodynamic equilibrium state, once the applied loads are released. The linear constitutive equations are adopted here to analyze relaxation-induced deformation and stresses, which are

$$\sigma_{\mathrm{g}} = K_{\mathrm{g}} \epsilon_{\mathrm{g}} \tag{4a}$$

for the grain, where ϵ_{g} and K_{g} are respectively the volumetric strain and bulk modulus of the grain, and

$$\sigma_{\mathrm{gb}}^{\parallel} = \sigma_{\mathrm{gb}}^{\parallel 0\delta} + \widehat{Y}_{\mathrm{gb}} (\varepsilon_{\mathrm{gb}}^{\parallel} + \nu_{\mathrm{gb}} \varepsilon_{\mathrm{gb}}^{\perp}), \tag{4b-1}$$

$$\sigma_{\mathrm{gb}}^{\perp} = \sigma_{\mathrm{gb}}^{\perp \delta} + \widehat{Y}_{\mathrm{gb}} \left[(1 - \nu_{\mathrm{gb}}) \varepsilon_{\mathrm{gb}}^{\perp} + 2\nu_{\mathrm{gb}} \varepsilon_{\mathrm{gb}}^{\parallel} \right], \tag{4b-2}$$

with

$$\widehat{Y}_{\rm gb}=\frac{Y_{\rm gb}}{1-v_{\rm gb}-2(v_{\rm gb})^2}, \tag{4b-3}$$

for the GBs, where $Y_{\rm gb}$ and $v_{\rm gb}$ are respectively the Young's modulus and Poisson's ratio of the GBs. Besides, there is a correlation of

$$L_0\left(1+\frac{1}{3}\epsilon_{\rm g}\right)+\Omega_0(1+\varepsilon_{\rm gb}^{\perp})=L_0(1+\varepsilon_{\rm gb}^{\parallel})+\Omega_0(1+\varepsilon_{\rm gb}^{\parallel}) \tag{4c}$$

in the deformation strains and the correlation ensures that the grain and GBs are always coherently bonded. In eq. (4c), the subscript "0" denotes the dimensions before GB segregation and relaxation.

The relaxation reduces the GB total eigenstress and induces deformation in both grain and GBs. The isothermal strain energy density $f_{\rm g}^{\rm m}$ in the grain and the change in the isothermal strain energy density $\Delta f_{\rm gb}^{\rm m}$ in the GBs are respectively

$$f_{\rm g}^{\rm m}=\int_0^{\varepsilon_{\rm g}}\sigma_g{\rm d}\epsilon_{\rm g}=\frac{K_{\rm g}}{2}(\epsilon_{\rm g})^2=\frac{1}{2}\sigma_{\rm g}\epsilon_{\rm g}, \tag{5a}$$

$$\begin{aligned}\Delta f_{\rm gb}^{\rm m}&=2\int_0^{\varepsilon_{\rm gb}^{\parallel}}\sigma_{\rm gb}^{\parallel}{\rm d}\varepsilon_{\rm gb}^{\parallel}+\int_0^{\varepsilon_{\rm gb}^{\perp}}\sigma_{\rm gb}^{\perp}{\rm d}\varepsilon_{\rm gb}^{\perp}\\&=2\sigma_{\rm gb}^{\parallel 0\delta}\varepsilon_{\rm gb}^{\parallel}+\sigma_{\rm gb}^{\perp\delta}\varepsilon_{\rm gb}^{\perp}\\&\quad+\widehat{Y}_{\rm gb}\left\{\left(\varepsilon_{\rm gb}^{\parallel}\right)^2+\frac{1-v_{\rm gb}}{2}\left(\varepsilon_{\rm gb}^{\perp}\right)^2+2v_{\rm gb}\varepsilon_{\rm gb}^{\perp}\varepsilon_{\rm gb}^{\parallel}\right\}.\end{aligned} \tag{5b}$$

Because of the opposite signs of $\sigma_{\rm gb}^{\parallel 0\delta}$ and $\varepsilon_{\rm gb}^{\parallel}$, the change in the isothermal strain energy density in the GBs is always negative, which is the driving force for relaxation. Thus, the isothermal mechanical energy of the system is given by

$$F^{\rm m}=F_{\rm g}^{\rm m}+F_{\rm gb}^{\rm m}=V_{\rm g0}\frac{K_{\rm g}}{2}(\epsilon_{\rm g})^2+V_{\rm gb0}\Delta f_{\rm gb}^{\rm m}. \tag{5c}$$

With the strain compatibility of

$$L_0\left(1+\frac{1}{3}\epsilon_{\rm g}\right)+\Omega_0(1+\varepsilon_{\rm gb}^{\perp})=L_0(1+\varepsilon_{\rm gb}^{\parallel})+\Omega_0(1+\varepsilon_{\rm gb}^{\parallel}),$$

eqs. (5a)-(5c) show that the isothermal mechanical energy is a function of $\varepsilon_{\rm gb}^{\parallel}$ and $\varepsilon_{\rm gb}^{\perp}$. The minimization of the isothermal mechanical energy requires

$$\frac{\partial F^{\rm m}}{\partial\varepsilon_{\rm gb}^{\parallel}}=0, \tag{6a}$$

$$\frac{\partial F^{\rm m}}{\partial\varepsilon_{\rm gb}^{\perp}}=0, \tag{6b}$$

which yields

$$L_0\sigma_{\rm g}+\frac{2\Omega_0}{1+\Omega_0/L_0}\sigma_{\rm gb}^{\parallel}=0, \tag{7a}$$

$$\sigma_{\rm g}=\sigma_{\rm gb}^{\perp}. \tag{7b}$$

Eq. (7a)[1] is called the generalized capillary equation and eq. (7b), as expected, is the traction continuity boundary condition along the normal direction of GBs. Then, using the constitutive eqs. (7a) and (7b) and the strain compatibility of eq. (4c), we have the strains of

$$\varepsilon_{\rm gb}^{\parallel}=-\frac{[3K_{\rm g}(L_0+\Omega_0)\Omega_0-2\widehat{Y}_{\rm gb}v_{\rm gb}L_0\Omega_0]\sigma_{\rm gb}^{\perp\delta}+2[3K_{\rm g}\Omega_0^2+\widehat{Y}_{\rm gb}(1-v_{\rm gb})L_0\Omega_0]\sigma_{\rm gb}^{\parallel 0\delta}}{\widehat{Y}_{\rm gb}\cdot\Psi}, \tag{8a}$$

$$\varepsilon_{\rm gb}^{\perp}=-\frac{[3K_{\rm g}(L_0+\Omega_0)^2+2\widehat{Y}_{\rm gb}L_0\Omega_0]\sigma_{\rm gb}^{\perp\delta}+2[3K_{\rm g}(L_0+\Omega_0)\Omega_0-2\widehat{Y}_{\rm gb}v_{\rm gb}L_0\Omega_0]\sigma_{\rm gb}^{\parallel 0\delta}}{\widehat{Y}_{\rm gb}\cdot\Psi}, \tag{8b}$$

$$\epsilon_{\rm g}=\frac{6[v_{\rm gb}(L_0+\Omega_0)\Omega_0+\Omega_0^2]\sigma_{\rm gb}^{\perp\delta}-6[2v_{\rm gb}\Omega_0^2+(1-v_{\rm gb})(L_0+\Omega_0)\Omega_0]\sigma_{\rm gb}^{\parallel 0\delta}}{\Psi}, \tag{8c}$$

with

$$\Psi=3K_{\rm g}[(1-v_{\rm gb})L_0^2+2(1+v_{\rm gb})L_0\Omega_0+3(1+v_{\rm gb})\Omega_0^2]+2\widehat{Y}_{\rm gb}(1-v_{\rm gb}-2v_{\rm gb}^2)L_0\Omega_0.$$

Eqs. (8a)-(8c) indicate that the strains depend all on the grain-size, the total GB eigenstress $\sigma_{\rm gb}^{\parallel 0\delta}$, which includes the GB eigenstress $\sigma_{\rm gb}^{\parallel 0}$ and the GB segregation induced eigenstress $\sigma_{\rm gb}^{\parallel\delta}$, and the elastic constants of the grain and GBs. Once the strains are determined, it is straightforward to calculate the stresses with the constitutive equations of eq. (4).

The derived equations can be applied to CG materials, where the value Ω_0/L_0 is sufficiently small. In this case, the generalized capillary equation still holds and is simplified to $L_0\sigma_{\rm g}+2\Omega_0\sigma_{\rm gb}^{\parallel}=0$. Approximately, we have zero hydrostatic stress in the grain

$$\sigma_{\rm g}=\sigma_{\rm gb}^{\perp}=0, \tag{9a}$$

and the GB stress of

$$\sigma_{\rm gb}^{\parallel}=\sigma_{\rm gb}^{\parallel 0\delta}-\frac{v_{\rm gb}}{(1-v_{\rm gb})}\sigma_{\rm gb}^{\perp\delta}. \tag{9b}$$

Then, the strain energy in the grain disappears and eq. (5b) is reduced to

1) The factor 2 is missing in eq. (17a) of our previous publication [38] and thereafter related equations in the publication.

$$\Delta f_{\rm gb}^{\rm m} = 2\sigma_{\rm gb}^{\parallel 0\delta}\varepsilon_{\rm gb}^{\parallel} + \widehat{Y}_{\rm gb}(\varepsilon_{\rm gb}^{\parallel})^2. \tag{9c}$$

If there is no GB segregation, such as in mono-element NG materials, eqs. (8a)-(8c) are reduced to

$$\varepsilon_{\rm gb}^{\parallel} = -\frac{2[3K_{\rm g}\Omega_0^2 + \widehat{Y}_{\rm gb}(1-\nu_{\rm gb})L_0\Omega_0]}{\widehat{Y}_{\rm gb}\cdot\Psi}\sigma_{\rm gb}^{\parallel 0}, \tag{10a}$$

$$\varepsilon_{gb}^{\perp} = -\frac{2[3K_{\rm g}(L_0+\Omega_0)\Omega_0 - 2\widehat{Y}_{\rm gb}\nu_{\rm gb}L_0\Omega_0]}{\widehat{Y}_{\rm gb}\cdot\Psi}\sigma_{\rm gb}^{\parallel 0}, \tag{10b}$$

$$\epsilon_{\rm g} = -\frac{6[2\nu_{\rm gb}\Omega_0^2 + (1-\nu_{\rm gb})(L_0+\Omega_0)\Omega_0]}{\Psi}\sigma_{\rm gb}^{\parallel 0}, \tag{10c}$$

respectively, and the mechanical energy densities per unit volume in the grain and in the GBs are still calculated with eqs. (5a) and (5b), respectively, with the change of $\sigma_{\rm gb}^{\parallel 0\delta} = \sigma_{\rm gb}^{\parallel 0}$ and $\sigma_{\rm gb}^{\perp\delta} = 0$.

2.2 Thermodynamic analysis

As illustred in Figure 2, a NG polycrystalline sample can be regarded to be built-up at a given temperature from its parent stress-free single crystalline counterpart. When it is just built-up without GB segregation and relaxation, the free energy of the grains will be the same as that inside their parent stress-free single crystalline counterpart, while the free energy of the 3D GBs will be higher than that, because the formation of GBs generates spontaneously the original excess free energy. Thus, the total free energy of the representative grain and associated GBs, before GB segregation and relaxation, takes the following form:

$$F^0 = \sum_i^k n_{{\rm s},i}\mu_{{\rm s},i} + \Gamma^0 = N\sum_i^k X_i\mu_{{\rm s},i} + \Gamma^0, \tag{11a}$$

where the superscript "0" denotes the newly built-up state, the subscript "s" denotes "single crystal", $N = \sum_i^k n_{{\rm s},i}$ is the total mole number, $n_{{\rm s},i}$, $X_i = n_{{\rm s},i}/N$, and $\mu_{{\rm s},i}$ are the mole number, the nominal mole fraction, and the chemical potential of element i, respectively, and Γ^0 is the original total excess free energy before GB segregation and relaxation. Eq. (11a) indicates that before GB segregation and relaxation, except of the gain of original total excess free energy Γ^0, the chemical potentials and the mole fractions in the grain and GBs are all the same as these in the corresponding single crystal, i.e.,

$$\mu_{{\rm g},i}^0 = \mu_{{\rm gb},i}^0 = \mu_{{\rm s},i}, \text{ for } i=1, 2, \ldots, k, \tag{11b}$$

$$x_{{\rm g},i}^0 = x_{{\rm gb},i}^0 = X_i, \text{ for } i=1, 2, \ldots, k. \tag{11c}$$

GB segregation and relaxation alter the chemical potentials and the mole fractions in the grain and GBs, and generate internal stress fields in the grain and GBs, although no external mechanical loads are applied on the studied NG material. The free energy of the polycrystal after GB segregation and relaxation is expressed by

$$F = F^{\rm c} + F^{\rm m} + \Gamma^0, \tag{12a}$$

where $F^{\rm m}$ is given by eq. (5c) and

$$F^{\rm c} = F_{\rm g}^{\rm c} + F_{\rm gb}^{\rm c} = \sum_i^k \mu_{{\rm g},i}n_{{\rm g},i} + \sum_i^k \mu_{{\rm gb},i}n_{{\rm gb},i}. \tag{12b}$$

Since the original total excess free energy is used in eq. (12a), the change in excess free energy is involved in $F^{\rm c} + F^{\rm m}$ and $N_i = n_{{\rm g},i} + n_{{\rm gb},i}$ for i=1, 2, …, k. The mole numbers $n_{{\rm g},i}$ and $n_{{\rm gb},i}$ after GB segregation and relaxation, however, differ correspondingly from the original mole numbers $n_{{\rm g},i}^0$ and $n_{{\rm gb},i}^0$ before GB segregation and relaxation. Letting $\Delta n_{{\rm gb},i} = n_{{\rm gb},i} - n_{{\rm gb},i}^0$ and $\Delta n_{{\rm g},i} = n_{{\rm g},i} - n_{{\rm g},i}^0$ denote the changes in mole numbers in the GBs and in the grain, respectively, we have $\Delta n_{{\rm g},i} = -\Delta n_{{\rm gb},i}$ due to the mass conservation of the studied closed system. Then, eq. (12b) is rewritten as:

$$F^{\rm c} = \sum_i^k \mu_{{\rm g},i}(n_{{\rm g},i}^0 - \Delta n_{{\rm gb},i}) + \sum_i^k \mu_{{\rm gb},i}(n_{{\rm gb},i}^0 + \Delta n_{{\rm gb},i}). \tag{12c}$$

The polycrystal after GB segregation and relaxation has the minimum free energy at thermodynamic equilibrium, which requires

$$\frac{\partial F}{\partial \Delta n_{{\rm gb},i}} = 0, \tag{13a}$$

$$\frac{\partial F}{\partial \varepsilon_{\rm gb}^{\parallel}} = 0, \tag{13b}$$

$$\frac{\partial F}{\partial \varepsilon_{\rm gb}^{\perp}} = 0. \tag{13c}$$

As expected, eq. (13a) yields the chemical equilibrium of $\mu_{gb,i} = \mu_{{\rm g},i}$ for i=1, 2, …, k, eq. (13b) leads to the generalized capillary equation of eq. (7a), and eq. (13c) gives the traction continuity boundary condition along the normal direction of the GBs. The chemical equilibrium demands that the chemical potential of each element in the GBs must equal to the corresponding chemical potential in the grain. When calculating the chemical potentials in a solid solution, one usually takes the chemical potentials of pure elements as the reference state. Due to the distinction between grain and GBs, however, the reference state of the chemical potential of a pure element in GBs is different from that of the same element in grain and this difference is called the standard Gibbs energy of segregation by Lejček and Hofmann [23]. The generalized McLean adsorption isotherm is developed based on the equal chemical potentials with different reference states [40].

The chemical potentials of element i (i=1, 2, …, k) at a constant temperature in the reference single crystal, crystalline grain, and GBs are respectively expressed in terms of "activity" as:

$$\mu_{{\rm s},i} = \mu_{{\rm s},i,0} + RT\ln a_{{\rm s},i}, \tag{14a}$$

$$\mu_{g,i} = \mu_{g,i,0} + RT\ln a_{g,i} - \overline{V}_{g,i}\sigma_g, \tag{14b}$$

$$\mu_{gb,i} = \mu_{gb,i,0} + RT\ln a_{gb,i} - \overline{V}_{gb,i}\frac{(2\sigma_{gb}^{\parallel}+\sigma_g)}{3}, \tag{14c}$$

where $\mu_{s,i,0} = \mu_{g,i,0}$ and $\mu_{gb,i}$ are the reference chemical potentials of pure element i in the stress-free grain and GBs, respectively, R is the gas constant, T denotes absolute temperature, and $a_{s,i}$, $a_{g,i}$ and $a_{gb,i}$ are the activities of element i in the reference single crystal, crystalline grain, and GBs, respectively. In eq. (14c), $\frac{(2\sigma_{gb}^{\parallel}+\sigma_g)}{3}$ is used to represent the GB hydrostatic stress. Then, using $\mu_{gb,i} = \mu_{g,i}$, we have [40]

$$a_{gb,i} = a_{g,i}\exp\left(\frac{\Delta\mu_{i,0} + \overline{V}_{gb,i}\frac{(2\sigma_{gb}^{\parallel}+\sigma_g)}{3} - \overline{V}_{g,i}\sigma_g}{RT}\right),$$

for i=1, 2, …, k, (15a)

where $\Delta\mu_{i,0} = -(\mu_{gb,i,0} - \mu_{g,i,0})$ is defined as the differentiation in reference chemical potential of element i, which is similar to the standard Gibbs energy of segregation [23]. Eq. (15a) is the thermodynamic GB segregation formula, which links the GB chemical composition to the chemical composition in the grain, as illustrated in the right side of Figure 1. Using the generalized capillary equation, we rewrite eq. (15a) as:

$$a_{gb,i} = a_{g,i}\exp\left(\frac{\Delta\mu_{i,0} + \frac{2\sigma_{gb}^{\parallel}}{L_0+\Omega_0}\left(\frac{L_0\overline{V}_{gb,i}}{3} + \Omega_0\overline{V}_{g,i}\right)}{RT}\right),$$

for i=1, 2, ..., k. (15b)

The partial molar volumes are usually positive. Thus, the mechanical energy will enhance the GB segregation, if the GB stress is tensile. The term of

$$\Delta\mu_{i,0} + \frac{2\sigma_{gb}^{\parallel}}{L_0+\Omega_0}\left(\frac{L_0\overline{V}_{gb,i}}{3} + \Omega_0\overline{V}_{g,i}\right)$$

might be called the generalized energy of segregation. In this sense, it might be more appropriate to call eq. (15a) or eq. (15b) the generalized Mclean adsorption isotherm. For CG samples, $\frac{\Omega_0}{L_0+\Omega_0} \to 0$ and $\frac{L_0}{L_0+\Omega_0} \to 1$ reduce eq. (15b) to

$$a_{gb,i}^{CG} = a_{g,i}^{CG}\exp\left(\frac{\Delta\mu_{i,0} + 2\overline{V}_{gb,i}\sigma_{gb}^{\parallel}/3}{RT}\right). \tag{15c}$$

The activities link directly to the chemical concentrations, which in turn determine the chemical eigenstrains and hence stresses. Therefore, eq. (15b) will be solved jointly with these stress equations of eqs. (4a) and (4b), as well as strain equations of eqs. (8a)-(8c).

Once the activities of elements at the GBs are determined from eq. (15b), the chemical concentrations and stresses in the grain and its GBs are determined, and then the total free energy after GB segregation and relaxation. Consider a NG alloy sample with a nominal mole fraction X_i (i=1, …, k), total mole number N, and volume V. When the single crystal is taken as the reference, the difference in the total free energy between the NG polycrystal, after GB segregation and relaxation, and single crystal is given by

$$\begin{aligned}\Delta F &= \sum_i^k(\mu_{g,i} - \mu_{s,i})N_i + V\left[f_{V,g}\frac{K_g}{2}(\epsilon_g)^2 + f_{V,gb}\Delta f_{gb}^{m}\right] + \Gamma^0 \\ &= \sum_i^k\left(RT\ln\frac{a_{g,i}}{a_{s,i}} - \overline{V}_{g,i}\sigma_g\right)N_i \\ &\quad + V\left[f_{V,g}\frac{K_g}{2}(\epsilon_g)^2 + f_{V,gb}\Delta f_{gb}^{m}\right] + \Gamma^0.\end{aligned} \tag{16a}$$

From eq. (16a), we have the difference in molar free energy, $\Delta\underline{F}$, and the difference in free energy density per unit volume, Δf:

$$\begin{aligned}\Delta\underline{F} &= \sum_i^k\left(RT\ln\frac{a_{g,i}}{a_{s,i}} - \overline{V}_{g,i}\sigma_g\right)X_i \\ &\quad + \frac{V}{N}\left[f_{V,g}\frac{K_g}{2}(\epsilon_g)^2 + f_{V,gb}\Delta f_{gb}^{m}\right] + \frac{\Gamma^0}{N},\end{aligned} \tag{16b}$$

$$\begin{aligned}\Delta f &= \frac{N}{V}\sum_i^k\left(RT\ln\frac{a_{g,i}}{a_{s,i}} - \overline{V}_{g,i}\sigma_g\right)X_i \\ &\quad + \left[f_{V,g}\frac{K_g}{2}(\epsilon_g)^2 + f_{V,gb}\Delta f_{gb}^{m}\right] + \frac{\Gamma^0}{V}.\end{aligned} \tag{16c}$$

The first and second terms in the right side of eqs. (16b) and (16c) represent the reductions in the chemical and mechanical free energies, respectively, while the third term in the right side of eqs. (16b) and (16c) is the gain of the excess free energy due to the formation of GBs. When the grain size gets smaller in a given total mass or a given total volume alloy, the GB and grain volumes will increase and decrease, respectively. Thus, the value of $\frac{\Gamma^0}{N}\left(\frac{\Gamma^0}{V}\right)$ will increase with the decrease in grain size and meanwhile the reductions in the chemical and mechanical free energies will increase also in different rates. Clearly, both differences in molar free energy and in free energy density per unit volume depend on the grain size, temperature, and the nominal concentration, and therefore each of them might be the right physical property to assess the thermal stability of NG alloys.

When studying interface segregation, the chemical potential of solute in the matrix phase is usually regarded unchanged due to the huge volume of the matrix phase. For the tiny grain size in NG alloys, GB segregation and relaxation also change the chemical potential and free energy in the grain. In this circumstance, the changed grain free energy

should be used as the background in the calculation of the excess free energy of the GBs, as did in the previous work [13,42]. With the original total excess free energy Γ^0, the free energies of the grain and GBs after GB segregation and relaxation are expressed, respectively, by

$$F_{\rm g} = F_{\rm g}^{\rm c} + F_{\rm g}^{\rm m} = \sum_i^k \mu_{{\rm g},i} n_{{\rm g},i} + V_{\rm g0}\frac{K_{\rm g}}{2}(\epsilon_{\rm g})^2 = N_{\rm g}\sum_i^k \mu_{{\rm g},i} x_{{\rm g},i} + V_{\rm g0}\frac{K_{\rm g}}{2}(\epsilon_{\rm g})^2, \tag{17a}$$

$$F_{\rm gb} = F_{\rm gb}^{\rm c} + F_{\rm gb}^{\rm m} = N_{\rm gb}\sum_i^k \mu_{{\rm gb},i} x_{{\rm gb},i} + V_{\rm gb0}\Delta f_{\rm gb}^{\rm m} + \Gamma^0, \tag{17b}$$

where $N_{\rm g} = \sum_i^k n_{{\rm g},i}$ and $x_{{\rm gb},i} = n_{{\rm g},i}/N_{\rm g}$ are the total mole number and the mole fraction of element i in the grain, respectively; $N_{\rm gb} = \sum_i^k n_{{\rm gb},i}$ and $x_{{\rm gb},i}$ are the total mole number and the mole fraction of element i in the GBs, respectively. After GB segregation and relaxation, the total excess free energy should be calculated with the reference that each element in the GBs has the same mole fraction as that in the grain. To meet this requirement, the mole number $n_{\rm gb,1}$ of solvent in the GBs, which is marked as element one in the present work, is taken to calculate the revised total mole number and mole number for element i (i=2, …, k) in the GBs via $\widehat{N}_{\rm gb} = n_{\rm gb,1}/x_{\rm g,1}$ and $\hat{n}_{{\rm gb},i} = \frac{n_{\rm gb,1}}{x_{\rm g,1}}x_{{\rm gb},i}$, respectively. GB segregation and relaxation causes the difference between $\widehat{N}_{\rm gb}$ and $N_{\rm gb}$ and the difference between $\hat{n}_{{\rm gb},i}$ and $n_{{\rm gb},i}$ for i=2, …, k. The total excess mole number alters the total mole number of the NG alloy from $N = N_{\rm g} + N_{\rm gb}$ to $\widehat{N}$ and thus the free energies of the NG alloy and the 3D GBs can be expressed by

$$F = \widehat{N}\sum_i^k \mu_{{\rm g},i} x_{{\rm g},i} + \left(V_{\rm g0} + V_{\rm gb0}\right)\frac{K_{\rm g}}{2}(\epsilon_{\rm g})^2 + \Gamma, \tag{17c}$$

$$F_{\rm gb} = \widehat{N}_{\rm gb}\sum_i^k \mu_{{\rm gb},i} x_{{\rm g},i} + V_{\rm gb0}\frac{K_{\rm g}}{2}(\epsilon_g)^2 + \Gamma, \tag{17d}$$

where Γ denotes the total excess free energy after GB segregation and relaxation. From eqs. (17b) and (17d), we have

$$\Gamma = \Gamma^0 + \sum_{i=2}^k \mu_{{\rm gb},i}\left(n_{{\rm gb},i} - \hat{n}_{{\rm gb},i}\right) + V_{\rm gb0}\left(\Delta f_{\rm gb}^{\rm m} - \frac{K_{\rm g}}{2}(\epsilon_{\rm g})^2\right). \tag{18a}$$

Dividing the total excess free energy of eq. (18a) by the GB area yields the GB energy density per unit GB area, γ,

$$\gamma = \gamma^0 + \sum_{i=2}^k \mu_{{\rm gb},i} c_i^{\rm gb,ex} + \Omega_0\left(\Delta f_{\rm gb}^{\rm m} - \frac{K_{\rm g}}{2}(\epsilon_{\rm g})^2\right), \tag{18b}$$

where $c_i^{\rm gb,ex} = \frac{n_{\rm gb,i} - \hat{n}_{{\rm gb},i}}{A}$ ($i \neq 1$) is the excess concentration per unit GB area of element i for i=2, …, k.

Although the theoretical analysis described above is very much general and can be applied to alloys with multiple elements, as long as the alloys are in solid solution, binary regular solid solution is taken in the following section as a typical example to illustrate the mechanical and thermodynamic analysis.

2.3 Binary regular solid solution

Without losing generality, element 2 is treated here as solute, i.e., the GB segregated species, because element 1 denotes solvent. For simplicity, we consider the typical segregation mode that solute atoms move from the grain interior to the GBs, while solvent atoms do not move at all, remaining their original mole numbers in the grain and GBs. Thus, the gained solute mole number in the GBs equals the lost solute mole number in the grain, i.e., $\Delta n_{\rm gb,2} = -\Delta n_{\rm g,2}$. Then, the solute mole fractions in the GBs and grain are given, respectively, by

$$x_{\rm gb} = \frac{XN_{\rm gb}^0 + \Delta n_{\rm gb,2}}{N_{\rm gb}^0 + \Delta n_{\rm gb,2}}, \tag{19a}$$

$$x_{\rm g} = \frac{XN_{\rm g}^0 - \Delta n_{\rm gb,2}}{N_{\rm g}^0 - \Delta n_{\rm gb,2}}. \tag{19b}$$

Hereafter the subscript "2" in the mole fractions is ignored for binary solid solutions. In this circumstance, the eigenstrain differentiation δ takes the explicit expression of

$$\delta = \left(\frac{\overline{V}_{\rm gb,2}}{V_{\rm gb0}} + \frac{\overline{V}_{\rm g,2}}{V_{\rm g0}}\right)\Delta n_{\rm gb,2}.$$

When the GBs and grain are both regular solutions, their activities take the expression of $a_i = x_i \cdot \exp\left[\frac{\omega}{RT}(1-x_i)^2\right]$, i=1, 2, with ω denoting the interaction energy between elements 1 and 2. Due to the finite number of segregated sites, eq. (15a) takes the following form, similar to the Mclean adsorption isotherm,

$$\frac{x_{\rm gb}}{1-x_{\rm gb}} \cdot \exp\left[\frac{\omega}{RT}\left(1-x_{\rm gb}\right)^2\right] = x_{\rm g}\exp\left[\frac{\omega}{RT}\left(1-x_{\rm g}\right)^2 + \frac{\Delta\mu_{2,0} + \frac{2\sigma_{\rm gb}^{\parallel}}{L_0+\Omega_0}\left(\frac{L_0\overline{V}_{\rm gb,2}}{3} + \Omega_0\overline{V}_{\rm g,2}\right)}{RT}\right]. \tag{20a}$$

Substituting eqs. (19a) and (19b) into eq. (20a) yields

$$\frac{\dfrac{XN_{\mathrm{gb}}^{0}+\Delta n_{\mathrm{gb},2}}{N_{\mathrm{gb}}^{0}+\Delta n_{\mathrm{gb},2}}}{1-\dfrac{XN_{\mathrm{gb}}^{0}+\Delta n_{\mathrm{gb},2}}{N_{\mathrm{gb}}^{0}+\Delta n_{\mathrm{gb},2}}}\cdot\exp\left[\frac{\omega}{RT}\left(1-\frac{XN_{\mathrm{gb}}^{0}+\Delta n_{\mathrm{gb},2}}{N_{\mathrm{gb}}^{0}+\Delta n_{\mathrm{gb},2}}\right)^{2}\right]$$

$$=\frac{XN_{\mathrm{g}}^{0}-\Delta n_{\mathrm{gb},2}}{N_{\mathrm{g}}^{0}-\Delta n_{\mathrm{gb},2}}\exp\left[\frac{\omega}{RT}\left(1-\frac{XN_{\mathrm{g}}^{0}-\Delta n_{\mathrm{gb},2}}{N_{\mathrm{g}}^{0}-\Delta n_{\mathrm{gb},2}}\right)^{2}+\frac{\Delta\mu_{2,0}+\dfrac{2\sigma_{\mathrm{gb}}^{\parallel}}{L_0+\Omega_0}\left(\dfrac{L_0\overline{V}_{\mathrm{gb},2}}{3}+\Omega_0\overline{V}_{\mathrm{g},2}\right)}{RT}\right]. \tag{20b}$$

In eq. (20b), the nominal concentration of solute X, the initial mole numbers N_{g}^{0} and N_{gb}^{0}, temperature T, the interaction energy ω, the differentiation in chemical potential $\Delta\mu_{2,0}$, the partial molar volumes $\overline{V}_{\mathrm{g},2}$ and $\overline{V}_{\mathrm{gb},2}$, the grain size L_0, and the GB thickness Ω_0 are all input parameters, thereby the relationship between $\Delta n_{\mathrm{gb},2}$ and $\sigma_{\mathrm{gb}}^{\parallel}$ is determined by eq. (20b). As described above, the eigenstrain differentiation δ depends on the value of $\Delta n_{\mathrm{gb},2}$, which gives the dependence of GB stress $\sigma_{\mathrm{gb}}^{\parallel}$ on $\Delta n_{\mathrm{gb},2}$. Thus, combining eq. (4b-1) with eq. (20b) allows one to determine $\Delta n_{\mathrm{gb},2}$ and $\sigma_{\mathrm{gb}}^{\parallel}$ simultaneously with more input parameters of the bulk modulus of the grain K_{g}, the GB elastic constants Y_{gb} and ν_{gb}, and the GB eigenstress $\sigma_{\mathrm{gb}}^{\parallel 0}$.

The $Ni_{1-X}Mo_X$ NG alloys are taken as an example to plot and illustrate the results of the theoretical analysis. The lattice constant of the $Ni_{1-X}Mo_X$ is estimated from the Vegard's law, $a_{\mathrm{Ni}_{1-X}\mathrm{Mo}_X}=Xa_{\mathrm{Mo}}+(1-X)a_{\mathrm{Ni}}$, where a denotes lattice constant. The values of a_{Mo}=0.3147 nm and a_{Ni}=0.3524 nm [9] are used in the present study and assumed to be independent of temperature. With the lattice constants, the partial molar volumes are estimated to be $\overline{V}_{\mathrm{Mo}}=4.514\times10^{-6}\,\mathrm{m^3/mol}$ and $\overline{V}_{\mathrm{Ni}}=6.583\times10^{-6}\,\mathrm{m^3/mol}$ for $X\leq20\%$. The molar volume of the $Ni_{1-X}Mo_X$ NG alloy is given by $\underline{V}=\dfrac{V}{N}=(1-X)\overline{V}_{\mathrm{Ni}}+X\overline{V}_{\mathrm{Mo}}$. The original mole numbers of the grain and GBs are calculated by $N_{\mathrm{g}}^{0}=\dfrac{V_{\mathrm{g0}}}{\underline{V}}$ and $N_{\mathrm{gb}}^{0}=\dfrac{V_{\mathrm{gb0}}}{\underline{V}}$, respectively. Then, the original mole numbers of Ni and Mo in the grain and GBs are $n_{\mathrm{g,Mo}}^{0}=XN_{\mathrm{g}}^{0}$ and $n_{\mathrm{g,Ni}}^{0}=(1-X)N_{\mathrm{g}}^{0}$, and $n_{\mathrm{gb,Mo}}^{0}=XN_{\mathrm{gb}}^{0}$ and $n_{\mathrm{gb,Ni}}^{0}=(1-X)N_{\mathrm{gb}}^{0}$, respectively. In the thermodynamic analysis, some GB properties are introduced and their values are not available at the moment, and should be determined from atomistic calculations and/or experimental investigations. For this reason, sevaral values of a property are used in the following numerical calculations and plots in order to illustrate the influence of the property on the thermal stability of NG alloys. A typical example is the differentiation in reference chemical potential of segregated element, which is similar to the standard Gibbs energy of segregation and can be separated into segregation enthalpy and segregation entropy. For a given NG alloy, the value of the differentiation in reference chemical potential of segregated element should be a constant, which is a statistic mean for various GBs in the NG alloy, at a certain temperature without any external mechanical loads. Here, various values of $\Delta\mu_{\mathrm{Mo},0}$ are investigated to show its role in GB segregation and relaxation. The input parameter values are listed in Table 1, which are all approximately treated to be constants in the present study.

The GB thickness of Ω_0 =1 nm is a widely acceptable value in the research field on NG materials [58,59]. For example, the GB thickness in nanocrystalline Pd-H was estimated to be (0.9±0.2) nm [49], and (1.1±0.2) nm [60]. The value of $\sigma_{\mathrm{gb}}^{\parallel 0}=1$ N/m is adopted here and this value is estimated based on that the GB eigenstresss is approximately half of the surface eigenstress, which are obtained from the previous atomic calculations [61,62]. Table A-1 in the book, *Theory of Dislocations* (J.P. Hirth and J. Lothe), indicates that GB energy ranges from 0.3 to 1 J/m^2 and the value of 1 J/m^2 is used here.

3 Results and discussion

3.1 Concentrations and stresses

With the input data of X = 0.05, T = 800 K, and $\overline{V}_{\mathrm{gb,Mo}}=0.7\overline{V}_{\mathrm{g,Mo}}$ for the differentiations in reference chemical potential of solute Mo, $\Delta\mu_{\mathrm{Mo},0}$ = 0, 5, 10, 20, 40, and 80 kJ/mol, Figure 3(a1) and (b1) show the Mo concentrations x_{gb} and x_{g} in the GBs and grain versus the grain size L_0/Ω_0, respectively. Since the value of $\Delta\mu_{\mathrm{Mo},0}$ represents the standard Gibbs energy of segregation, i.e., the trap depth of GBs to solute atoms, the larger the value of $\Delta\mu_{\mathrm{Mo},0}$ is, the higher the GB solute concentration and the lower the solute concentration in the grain will be, as shown in Figure 3(a1) and (b1), respectively. For the highest value of $\Delta\mu_{\mathrm{Mo},0}$ = 80 kJ/mol, the severe GB segregation is able to take almost all solute Mo atoms to the GBs when the grain size is smaller than $60L_0/\Omega_0$,

Table 1 The input parameter values

Parameter values (units)	Parameter values (units)
$\overline{V}_{g,Mo}$: 4.514×10^{-6} m^3/mol	$\overline{V}_{gb,Mo}=y\overline{V}_{g,Mo}$ and y=0.9, 0.7, 0.5
K_g: 202 GPa [56]	X: 0.005, 0.01, 0.02, 0.05, 0.1, 0.2
K_{gb}: 160 GPa [56]	$\Delta\mu_{Mo,0}$: 0, 5, 10, 20, 40, 80 kJ/mol
ν_{gb}: 0.32 [56]	T: 500, 800, 1100, 1400 K
ω: −10 kJ/mol	Ω_0: 1 nm
$\sigma_{gb}^{\parallel 0}$: 1 GPa	L_0: 3-10000 (Ω_0)
γ^0: 1 J/m^2	$\mu_{g,Mo,0}=-7746.302+131.9197T-23.56414T\ln T-3.443396\times10^{-3}T^2+0.566283\times10^{-6}T^3+\frac{65812}{T}-0.130927\times10^{-9}T^4+15200+0.63T$ J/mol [57]

thereby leaving nearly no Mo atoms in the grain ($x_g\leq$ 0.0012). If the grain size is larger than $1800L_0/\Omega_0$, the solute concentration in the grain will be higher than x_g= 0.0473 and gradually approaches the nominal solute concentration, while the GB solute concentration x_{gb}= 0.6501 will almost approach its saturated value x_{gb}= 0.6571 at $10^4L_0/\Omega_0$, as illustrated in Figure 3(a1) and (b1). It is interesting that even $\Delta\mu_{Mo,0}$= 0 the GB eigenstress can also cause GB segregation, which gives the maximum value of x_{gb}= 0.0599 at $\sigma_{gb}^{\parallel 0}$= 1.0 GPa.

Temperature plays a significant role in GB segregation, as indicated by eqs. (20a) and (20b). With the input data of X = 0.05, $\Delta\mu_{Mo,0}$= 20 kJ/mol, and $\overline{V}_{gb,Mo}=0.7\overline{V}_{g,Mo}$ for the temperatures of T=500, 800, 1100, and 1400 K, Figure 3(a2) and (b2) show the Mo concentrations x_{gb} and x_g in the GBs and grain versus the grain size L_0/Ω_0, respectively. As expected, the lower the temperature is, the more severe GB segregation will be. The almost saturated GB Mo concentrations at $100L_0/\Omega_0$ are 0.2709, 0.2210, 0.1844, 0.1579 at temperatures of 500, 800, 1100, and 1400 K, respectively, indicating that lowering temperature from 1400 to 500 K increases the solute concentration in the GBs by 1.72 times.

The value of the partial molar volume of solute in the GBs depends on the GB type and microstructure, while the statistical mean of GB partial molar volume should be used in the present work. The GB partial molar volume of solute affects the GB segregation, GB and grain concentrations, especially the almost saturated GB concentration, as shown in Figure 3(a3) and (b3). A smaller value of partial molar volume of solute in GBs implies a smaller chemical strain induced by GB segregation, thereby yielding a higher GB concentration. With the input data of $\Delta\mu_{Mo,0}$= 20 kJ/mol, T = 800 K, and $\overline{V}_{gb,Mo}=0.7\overline{V}_{g,Mo}$ for the nominal concentrations of X = 0.005, 0.01, 0.02, 0.05, 0.1, and 0.2, Figure 3(a4) and (b4) exhibit the Mo concentrations x_{gb} and x_g in the GBs and grain versus the grain size L_0/Ω_0, respectively. As indicated by eq. (20b), the concentration x_{gb}, calculated by the generalized McLean adsorption isotherm, links directly to the concentration x_g, and both are related to the nominal concentration X. For a given nominal concentration, the concentration x_{gb} monotonically increases with the grain size and gradually approaches a steady value. When the grain size is smaller, a relatively larger portion of solute atoms will move to the GBs from the grain, which makes the concentration x_g much lower than the nominal concentration X, as shown in Figure 3(b4). The supply of solute atoms to GB segregation grows up with the increase in grain size such that both concentrations x_{gb} and x_g increase with the grain size.

With the same input data as these in plotting Figure 3(a1) and (b1), Figure 4(a1) and (b1) show the elastic GB in-plane stress $\sigma_{gb}^{\parallel}$ and elastic grain hydrostatic stress σ_g versus the grain size L_0/Ω_0, respectively. After GB segregation and relaxation, the GB in-plane stress $\sigma_{gb}^{\parallel}$ varies from positive to negative and gradually approaches the limit of $\sigma_{gb}^{\parallel}=\sigma_{gb}^{\parallel 0\delta}-\frac{\nu_{gb}}{(1-\nu_{gb})}\sigma_{gb}^{\perp\delta}$ for CG samples. The limit depends on the value of standard Gibbs energy of segregation $\Delta\mu_{Mo,0}$. The larger the value of $\Delta\mu_{Mo,0}$ is, the higher the compressive limit of the GB in-plane stress $\sigma_{gb}^{\parallel}$ will be, as shown in Figure 4(a1). Figure 4(b1) indicates that for $\Delta\mu_{Mo,0}$= 0 and 5 kJ/mol, the compressive grain stress σ_g monotonically decreases its magnitude and gradually disappears due to the reason that as the grain size gets larger and larger, the stiffness of the sample will become stronger and stronger, which makes the relaxation harder and harder. When the value of $\Delta\mu_{Mo,0}$ is higher than 10 kJ/mol, grain stress σ_g will vary from compressive to tensile, reach a maximum tensile value, and then decrease gradually to zero. The maximum tensile stresses of σ_g are 0.0145, 0.1327, 0.2977, and 0.4057 GPa for the values of $\Delta\mu_{Mo,0}$ = 10, 20, 40, and 80 kJ/mol, respectively. This is

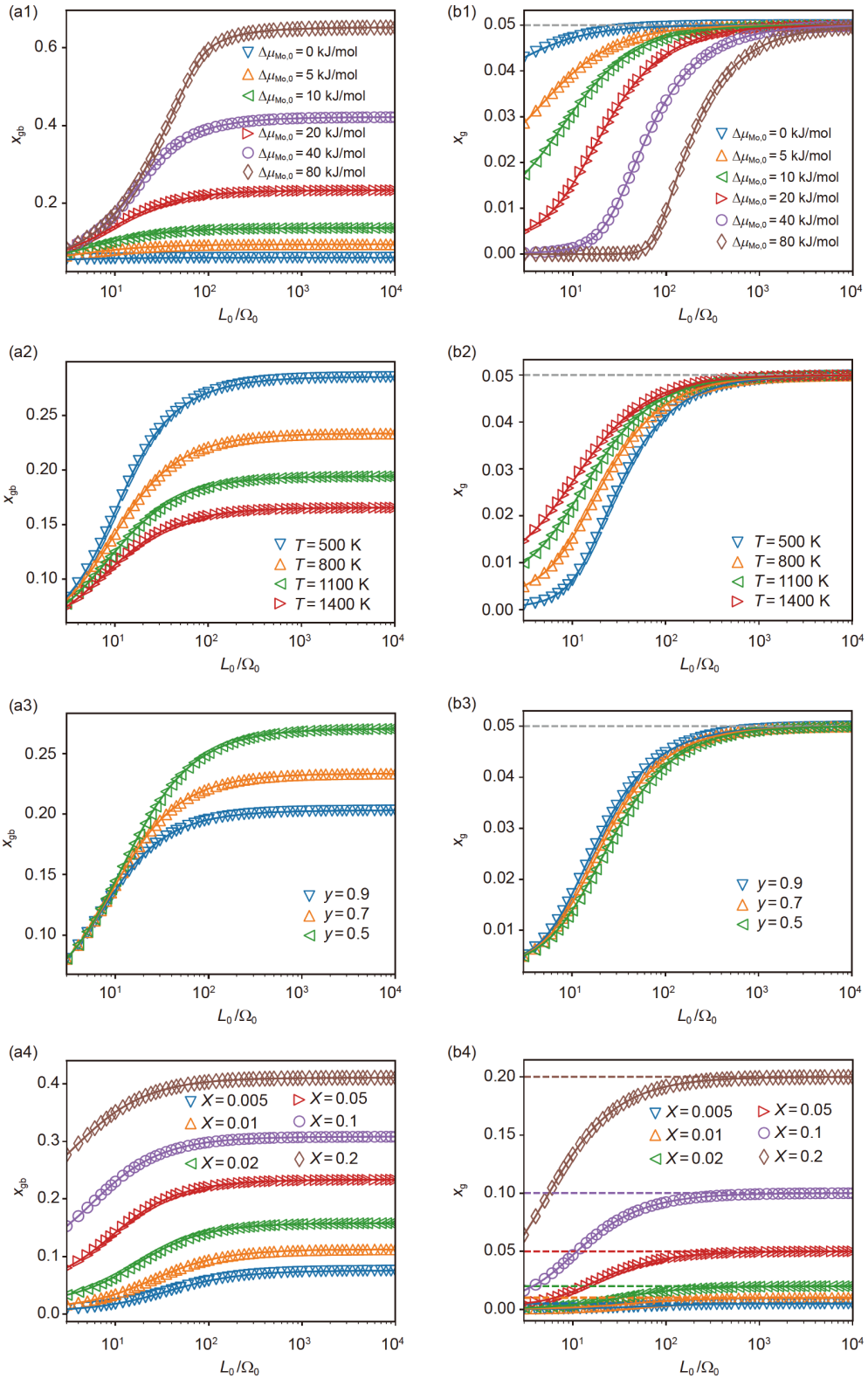

Figure 3 (Color online) Solute Mo concentrations x_{gb} in the GBs (a1)-(a4) and x_g in the grain (b1)-(b4) versus the grain size L_0/Ω_0, where the input data are X=0.05, T=800 K, and $\overline{V}_{gb,Mo} = 0.7\overline{V}_{g,Mo}$ for $\Delta\mu_{Mo,0}$ = 0, 5, 10, 20, 40, and 80 kJ/mol in (a1), (b1); X=0.05, $\Delta\mu_{Mo,0}$= 20 kJ/mol, and $\overline{V}_{gb,Mo} = 0.7\overline{V}_{g,Mo}$ for T= 500, 800, 1100, and 1400 K in (a2), (b2); $\Delta\mu_{Mo,0}$= 20 kJ/mol, T=800 K, and X= 0.05 for $\overline{V}_{gb,Mo}$= 0.9, 0.7, and 0.5 $\overline{V}_{g,Mo}$ in (a3), (b3); and $\Delta\mu_{Mo,0}$= 20 kJ/mol, T= 800 K, and $\overline{V}_{gb,Mo} = 0.7\overline{V}_{g,Mo}$ for X= 0.005, 0.01, 0.02, 0.05, 0.1, and 0.2 in (a4), (b4). The horizontal dashed lines in (b1)-(b4) show the nominal concentrations.

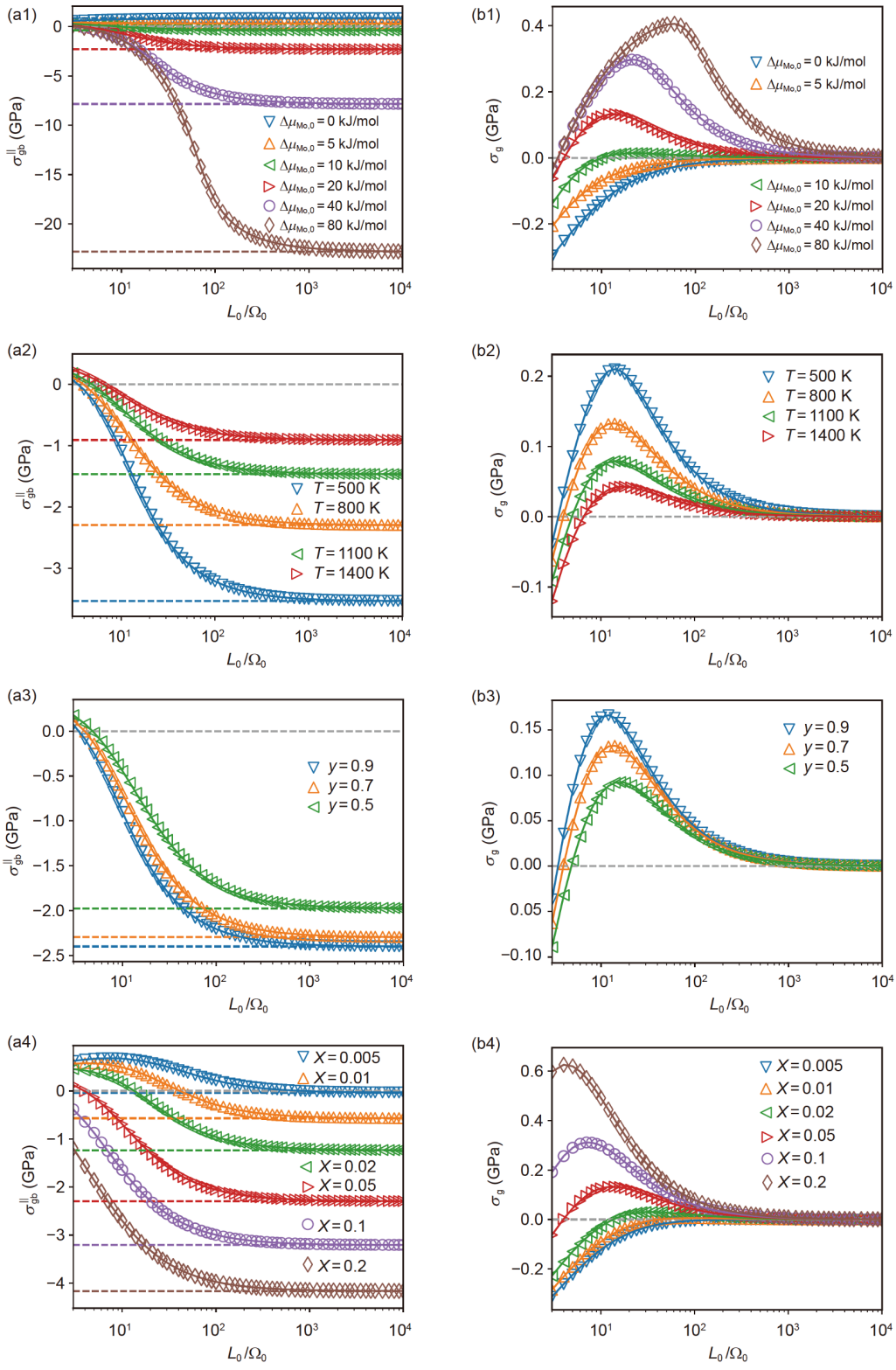

Figure 4 (Color online) GB in-plane stress $\sigma_{gb}^{\parallel}$ (a1)-(a4) and grain hydrostatic stress σ_g (b1)-(b4) versus the grain size L_0/Ω_0; where the input data are X=0.05, T=800 K, and $\overline{V}_{gb,Mo} = 0.7\overline{V}_{g,Mo}$ for $\Delta\mu_{Mo,0}$ = 0, 5, 10, 20, 40, and 80 kJ/mol in (a1), (b1); X=0.05, $\Delta\mu_{Mo,0}$ = 20 kJ/mol, and $\overline{V}_{gb,Mo} = 0.7\overline{V}_{g,Mo}$ for T= 500, 800, 1100, and 1400 K in (a2), (b2); $\Delta\mu_{Mo,0}$ = 20 kJ/mol, T=800 K, and X= 0.05 for $\overline{V}_{gb,Mo}$ = 0.9, 0.7, and 0.5 $\overline{V}_{g,Mo}$ in (a3), (b3); and $\Delta\mu_{Mo,0}$ = 20 kJ/mol, T= 800 K, and $\overline{V}_{gb,Mo} = 0.7\overline{V}_{g,Mo}$ for X= 0.005, 0.01, 0.02, 0.05, 0.1, and 0.2 in (a4), (b4). The horizontal dashed lines show the GB and grain stresses for CG alloys.

because a larger value of $\Delta\mu_{\mathrm{Mo},0}$ causes more severe GB segregation. When more solute atoms are segregated in the GBs, the GBs have stronger tendency to expand, while the grain puts constraint against the GB expansion. As a result, the elastic GB and grain stresses become compressive and tensile, respectively, and the tensile grain stress reaches its maximum when the GB segregation is almost saturated. If the grain size increases further after the maximum grain stress, the enhancement in GB segregation will be lower than the increase in relaxation constraint stiffness, thereby making the elastic deformation of the grain less and less, and the elastic grain stress approach finally to zero.

The effect of temperature on the GB segregation is also exhibited by the variations of elastic GB and grain stresses $\sigma_{\mathrm{gb}}^{\parallel}$ and σ_{g}. With the input data of X = 0.05, $\Delta\mu_{\mathrm{Mo},0}$= 20 kJ/mol, and $\overline{V}_{\mathrm{gb,Mo}} = 0.7\overline{V}_{\mathrm{g,Mo}}$ for temperatures of T = 500, 800, 1100, and 1400 K, Figure 4(a2) and (b2) show the elastic GB in-plane stress $\sigma_{\mathrm{gb}}^{\parallel}$ and grain stress σ_{g} versus the grain size L_0/Ω_0, respectively. Since $\sigma_{\mathrm{gb}}^{\delta} = -\frac{1}{3}K_{\mathrm{gb}}\delta$ and the differentiation δ of the chemical composition induced eigenstrains depends strongly on temperature, the limit of $\sigma_{\mathrm{gb}}^{\parallel} = \sigma_{\mathrm{gb}}^{\parallel 0\delta} - \frac{\nu_{\mathrm{gb}}}{(1-\nu_{\mathrm{gb}})}\sigma_{\mathrm{gb}}^{\perp\delta}$ for CG samples varies considerably with temperature, which values are −3.5357, −2.2962, −1.4653, and −0.9058 GPa for temperatures of 500, 800, 1100, and 1400 K, respectively, as shown in Figure 4(a2). The maximum tensile stresses of σ_{g} are 0.2098, 0.1327, 0.0790, 0.0427 GPa for temperatures of 500, 800, 1100, and 1400 K, respectively.

Figure 4(a3) and (b3) show the GB and grain stresses $\sigma_{\mathrm{gb}}^{\parallel}$ and σ_{g} as a function of grain size for the partial molar volumes of $\overline{V}_{\mathrm{gb,Mo}}$ = 0.9, 0.7, and 0.5 $\overline{V}_{\mathrm{g,Mo}}$, respectively, where the input data are $\Delta\mu_{\mathrm{Mo},0}$= 20 kJ/mol, T = 800 K, and X = 0.05. Along with the increase in grain size, the GB stress $\sigma_{\mathrm{gb}}^{\parallel}$ varies monotonically from tensile to compressive. The maximum compressive $\sigma_{\mathrm{gb}}^{\parallel}$, depending on the partial molar volumes of $\overline{V}_{\mathrm{gb,Mo}}$, are −2.400, −2.2962, and −1.9747 GPa for $\overline{V}_{\mathrm{gb,Mo}}$ =0.9, 0.7, and 0.5$\overline{V}_{\mathrm{g,Mo}}$, respectively. Obviously, a smaller value of $\overline{V}_{\mathrm{gb,Mo}}$ means that the GBs provide relatively larger space to accommodate the segregated solute atoms, thereby generating a lower value of the maximum compressive GB stress $\sigma_{\mathrm{gb}}^{\parallel}$. However, the curves of σ_{g} versus L_0/Ω_0 exhibit peaks and these parks are all tensile. The tensile peaks of σ_{g} are 0.1662, 0.1327, and 0.0926 GPa for $\overline{V}_{\mathrm{gb,Mo}}$ = 0.9, 0.7, and 0.5 $\overline{V}_{\mathrm{g,Mo}}$, respectively, as shown in Figure 4(b3), indicating that a larger value of $\overline{V}_{\mathrm{gb,Mo}}$ corresponds a higher value of the tensile peak stress of σ_{g}. With the input data of $\Delta\mu_{\mathrm{Mo},0}$= 20 kJ/mol, T = 800 K, and $\overline{V}_{\mathrm{gb,Mo}} = 0.7\overline{V}_{\mathrm{g,Mo}}$ for the nominal concentrations of X = 0.005, 0.01, 0.02, 0.05, 0.1, and 0.2, Figure 4(a4) and (b4) exhibit the GB and grain stresses $\sigma_{\mathrm{gb}}^{\parallel}$ and σ_{g} versus grain size, respectively. Under these conditions, the variations of $\sigma_{\mathrm{gb}}^{\parallel}$ and σ_{g} versus L_0/Ω_0 shown in Figure 4(a4) and (b4) are correspondingly similar to these shown in Figure 4(a1) and (b1). When the nominal concentration X is equal to and higher than 0.02, a tensile grain stress peak appears. The grain stress peaks are located at (0.0306 GPa, $35L_0/\Omega_0$), (0.1327 GPa, $14L_0/\Omega_0$), (0.3117 GPa, $7L_0/\Omega_0$), and (0.6259 GPa, $4\,L_0/\Omega_0$) for X=0.02, 0.05, 0.1, and 0.2, respectively.

In brief, the results shown in Figure 4(a1)-(a4) and (b1)-(b4) indicate the high elastic stresses at the magnitude of GPa could be generated in GBs and grains by GB segregation and relaxation.

3.2 The difference in molar free energy

Eq. (16b) gives the difference in molar free energy with the grain size. To emphasize the role of stress in the difference of molar free energy, eq. (16b) is rewritten as:

$$\Delta\underline{F} = \Delta\underline{F}_1 + \Delta\underline{F}_2 + \underline{V}\frac{\Gamma^0}{(L_0+\Omega_0)^3}, \tag{21a}$$

$$\Delta\underline{F}_1 = (1-X)RT\ln\frac{a_{\mathrm{g,Ni}}}{a_{\mathrm{s,Ni}}} + XRT\ln\frac{a_{\mathrm{g,Mo}}}{a_{\mathrm{s,Mo}}}, \tag{21b}$$

$$\Delta\underline{F}_2 = -\sigma_g\underline{V}^* + \underline{V}\left[f_{V,\mathrm{g}}\frac{K_{\mathrm{g}}}{2}(\varepsilon_{\mathrm{g}})^2 + f_{V,\mathrm{gb}}\Delta f_{\mathrm{gb}}^{\mathrm{m}}\right], \tag{21c}$$

where $\underline{V}^* = X\overline{V}_{\mathrm{g,Mo}} + (1-X)\overline{V}_{\mathrm{g,Ni}}$, $\Delta\underline{F}_1$ epitomizes the purely chemical contribution, viz. purely contribution from the difference in chemical composition due to GB segregation, and $\Delta\underline{F}_2$ represents the contribution from all stress involved terms. Clearly, the term of $\underline{V}\frac{\Gamma^0}{(L_0+\Omega_0)^3}$ is always positive and increases monotonically with the decrease in grain size, which is the driving force for grain growth or the resistance to the thermal stability of NG alloys. Both $\Delta\underline{F}_1$ and $\Delta\underline{F}_2$ may be negative and hence make contributions in the thermal stability of NG alloys. Figure 5(a1)-(a4) show the curves of $\Delta\underline{F}$ versus L_0/Ω_0, where the input data are correspondingly the same as these in Figure 4(a1)-(a4). If the grain size is sufficiently large, the value of $\Delta\underline{F}$ nulls, thereby indicating that CG alloys are thermally stable. When the standard Gibbs energy of segregation is lower than 20 kJ/mol, $\Delta\underline{F}$ will monotonically increase with the decrease in grain size, while if the standard Gibbs energy of segregation is equal to and higher than 20 kJ/mol, $\Delta\underline{F}$ will first decrease, reach a minimum value, and then increase with the decrease in grain size,

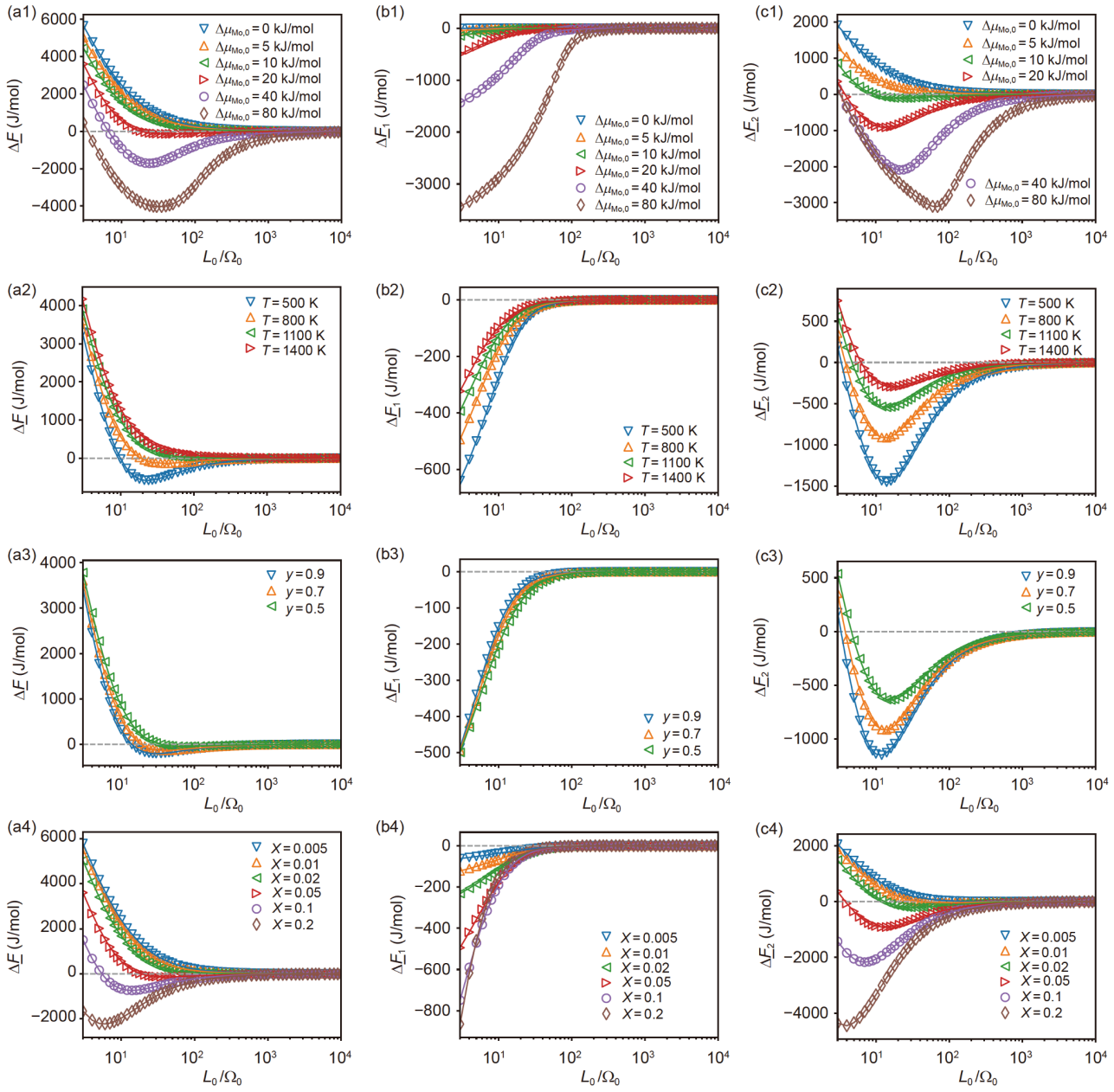

Figure 5 (Color online) As functions of grain size L_0/Ω_0, the difference in molar free energy, between a NG polycrystalline alloy and its reference single crystal with same chemical composition, the difference $\Delta\underline{F}$ (a1)-(a4), the purely concentration contribution $\Delta\underline{F}_1$ (b1)-(b4), and the contribution from the stress-involved terms $\Delta\underline{F}_2$ (c1)-(c4); where the input data are X=0.05, T=800 K, and $\overline{V}_{\mathrm{gb,Mo}} = 0.7\overline{V}_{\mathrm{g,Mo}}$ for $\Delta\mu_{\mathrm{Mo,0}}$ = 0, 5, 10, 20, 40, and 80 kJ/mol in (a1), (b1), (c1); X=0.05, $\Delta\mu_{\mathrm{Mo,0}}$ = 20 kJ/mol, and $\overline{V}_{\mathrm{gb,Mo}} = 0.7\overline{V}_{\mathrm{g,Mo}}$ for T= 500, 800, 1100, and 1400 K in (a2), (b2), (c2); $\Delta\mu_{\mathrm{Mo,0}}$ = 20 kJ/mol, T=800 K, and X= 0.05 for $\overline{V}_{\mathrm{gb,Mo}}$ = 0.9, 0.7, and 0.5 $\overline{V}_{\mathrm{g,Mo}}$ in (a3), (b3), (c3); and $\Delta\mu_{\mathrm{Mo,0}}$ = 20 kJ/mol, T=800 K, and $\overline{V}_{\mathrm{gb,Mo}} = 0.7\overline{V}_{\mathrm{g,Mo}}$ for X= 0.005, 0.01, 0.02, 0.05, 0.1, and 0.2 in (a4), (b4), (c4). The horizontal dashed lines show $\Delta\underline{F} = 0$, $\Delta\underline{F}_1 = 0$, and $\Delta\underline{F}_2 = 0$.

as shown in Figure 5(a1), indicating that in a range of grain size, the NG alloys are thermally stable, and the higher the value of $\Delta\mu_{\mathrm{Mo,0}}$ is, the larger the thermally stable range will be. The results imply that there exists a critical value of the standard Gibbs energy of segregation, below which NG alloys are thermally instable. This critical value depends on other parameters of temperature, partial molar volume of solute in GBs, and nominal solute concentration. Figure 5(a2) and (a3) show the roles of temperature and partial molar volume of solute in GBs in the thermal stability, respectively. As expected, NG alloys will be stable at low temperatures. For given values of $\Delta\mu_{\mathrm{Mo,0}}$, X, and $\overline{V}_{\mathrm{gb,Mo}}$, there is a critical temperature, above which the NG alloys are thermally instable and below which there is a thermally stable range of

grain size. The thermally stable range of grain size is bigger when temperature is lower, as shown in Figure 5(a2). If the partial molar volume of solute in GBs is smaller, e.g., $\overline{V}_{\mathrm{gb,Mo}} = 0.5\overline{V}_{\mathrm{g,Mo}}$, the difference in free energy $\Delta\underline{F}$ will monotonically increase with the decrease in grain size, while if the partial molar volume of solute in GBs is larger, e.g., $\overline{V}_{\mathrm{gb,Mo}} = 0.9\overline{V}_{\mathrm{g,Mo}}$, there will be a range in grain size during which $\Delta\underline{F}$ is negative, as shown in Figure 5(a3), meaning that NG alloys are thermally stable in this range. Nominal concentration is an easily adjusted parameter in the design and control of thermally stable NG alloys. Figure 5(a4) shows the role of nominal concentration in the thermally stability of the $Ni_{1-X}Mo_X$ NG alloys. For the input parameters of $\Delta\mu_{\mathrm{Mo},0}$= 20 kJ/mol, T = 800 K, and $\overline{V}_{\mathrm{gb,Mo}} = 0.7\overline{V}_{\mathrm{g,Mo}}$, the nominal concentration X = 0.2 is able to thermally stabilize the NG alloys in the entire range of grain size. On contrast, when the nominal concentration is equal to and lower than 0.02, only CG alloys are thermally stable.

To illustrate the contributions of $\Delta\underline{F}_1$ and $\Delta\underline{F}_2$, Figure 5(b1)-(b4) and (c1)-(c4) show the curves of $\Delta\underline{F}_1$ and $\Delta\underline{F}_2$ versus L_0/Ω_0, respectively, where the input data are correspondingly the same as these in Figure 5(a1)-(a4). For all the calculated cases, the values of $\Delta\underline{F}_1$ decrease with the reduction of grain size, as illustrated in Figure 5(b1)-(b4). The decrease of $\Delta\underline{F}_1$ is more significant if the value of $\Delta\mu_{\mathrm{Mo},0}$ is higher, the temperature is lower, the GB partial molar volume of solute is smaller, and/or the nominal solute concentration is larger. The result indicates that the purely chemical contribution via GB segregation reduces the free energy of the studied NG alloy. Except for the $\Delta\underline{F}_1$ values with $\Delta\mu_{\mathrm{Mo},0}$= 20 and 40 kJ/mol shown in Figure 5(b1), the magnitude of rest $\Delta\underline{F}_1$ values is less than 1000 J/mol, as shown in Figure 5(b1)-(b4). However, the behavior of $\Delta\underline{F}_2$ is completely different from that of $\Delta\underline{F}_1$. With the same input data of X = 0.05, T = 800 K, and $\overline{V}_{\mathrm{gb,Mo}} = 0.7\overline{V}_{\mathrm{g,Mo}}$, Figure 5(c1) illustrates that with the reduction in grain size, the value of $\Delta\underline{F}_2$ monotonically increases for $\Delta\mu_{\mathrm{Mo},0}$= 0 and 5 kJ/mol, and the increase is more significant when $\Delta\mu_{\mathrm{Mo},0}$ is smaller and the grain size is tinier; while for $\Delta\mu_{\mathrm{Mo},0}$= 10, 20, 40, and 80 kJ/mol, $\Delta\underline{F}_2$ decreases first with the reduction in grain size, reaches a minimum, and then increases. Comparing Figure 5(c1) with Figure 5(a1) exhibits that the curve shape of $\Delta\underline{F}$ versus L_0/Ω_0 is similar to that of $\Delta\underline{F}_2$ versus L_0/Ω_0, thereby implying that $\Delta\underline{F}_2$ is the major contributor to the thermal stability of NG alloys. The similarity in the curve shapes with the same input data in calculations is also illustrated between Figure 5(c2)-(c4) and (a2)-(a4), respectively. Furthermore, for most of the calculated cases, the magnitude of the largest values of $\Delta\underline{F}_2$ is higher than that of $\Delta\underline{F}_1$. The results exhibit that the contribution from $\Delta\underline{F}_2$ to the reduction of molar free energy is much bigger than that from $\Delta\underline{F}_1$.

In brief, the plots in Figure 5(a1)-(a4), (b1)-(b4), (c1)-(c4) illustrate that the molar free energy of a NG alloy under certain conditions is lower than that of referenced single crystal with the same nominal concentration, which provides the thermodynamic foundation of thermal stability of NG alloys. The stress involved molar free energy plays a more significant role than purely chemical molar free energy in the thermal stability of NG alloys.

3.3 The reduction of excess GB free energy

The excess concentration per unit GB area of solute Mo is calculated by $c_{\mathrm{Mo}}^{\mathrm{gb,ex}} = \dfrac{n_{\mathrm{gb,Mo}} - \hat{n}_{\mathrm{gb,Mo}}}{A}$, where A is the GB area and $\hat{n}_{\mathrm{gb,Mo}} = \dfrac{n_{\mathrm{gb,Ni}}}{x_{\mathrm{g,Ni}}} x_{\mathrm{gb,Mo}}$. Figure 6(a1)-(a4) show the curves of $c_{\mathrm{Mo}}^{\mathrm{gb,ex}}$ versus L_0/Ω_0, where the input data are correspondingly the same as these in Figure 5(a1)-(a4). The standard Gibbs energy of segregation $\Delta\mu_{\mathrm{Mo},0}$ plays a considerable role in the GB segregation. The higher the value of $\Delta\mu_{\mathrm{Mo},0}$ is, the higher the excess concentration $c_{\mathrm{Mo}}^{\mathrm{gb,ex}}$ will be, as illustrated in Figure 6(a1). When the grain size is too small, no sufficient solute atoms can be supplied from the grain and hence the influence of $\Delta\mu_{\mathrm{Mo},0}$ looks less on $c_{\mathrm{Mo}}^{\mathrm{gb,ex}}$. Since the term of $\Delta\mu_{\mathrm{Mo},0}/T$ appears together in the segregation formula of eq. (20b), lowering temperature is equivalent to enhancing the standard Gibbs energy of segregation. Figure 6(a2) indicates that the lower the temperature is, the higher the excess concentration $c_{\mathrm{Mo}}^{\mathrm{gb,ex}}$ will be. In addition to temperature, the GB partial molar volume of $\overline{V}_{\mathrm{gb,Mo}}$ affects the level of excess concentration because it varies the GB stress and the grain stress, as plotted in Figure 4(a3) and (b3). As predicted from the generalized Mclean adsorption isotherm of eq. (20b), the GB concentration depends on the nominal concentration, which results in the nominal concentration-dependent excess concentration, as shown in Figure 6(a4), indicating that a higher nominal concentration leads to a higher excess concentration.

The GB segregation and relaxation lower the excess GB free energy. For the studied binary alloy, eq. (18b) takes the form of

$$\gamma = \gamma^0 + \left(\mu_{\mathrm{g,Mo},0} + RT\ln a_{\mathrm{g,Mo}}\right)c_{\mathrm{Mo}}^{\mathrm{gb,ex}} + \Omega_0\left(\Delta f_{\mathrm{gb}}^{\mathrm{m}} - \frac{K_{\mathrm{g}}}{2}(\epsilon_{\mathrm{g}})^2\right). \tag{22}$$

Figure 6(b1)-(b4) show the curves of γ versus L_0/Ω_0, where the input data are correspondingly the same as these in

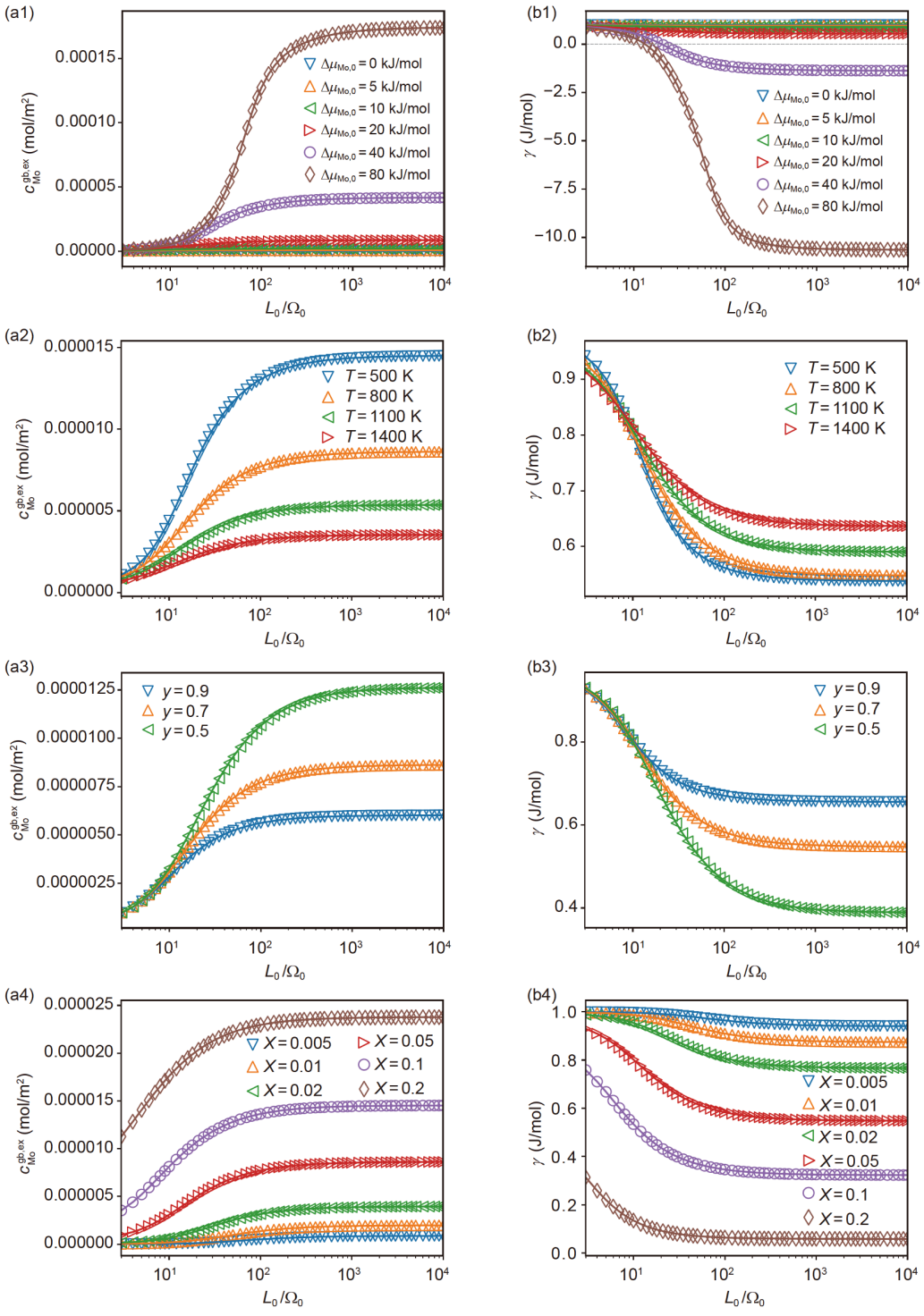

Figure 6 (Color online) (a1)-(a4) The excess concentration per unit GB area of solute versus the grain size L_0/Ω_0 and (b1)-(b4) the excess GB free energy density per unit GB area versus the grain size L_0/Ω_0; where the input data are X=0.05, T=800 K, and $\overline{V}_{gb,Mo} = 0.7\overline{V}_{g,Mo}$ for $\Delta\mu_{Mo,0}$= 0, 5, 10, 20, 40, and 80 kJ/mol in (a1), (b1); X=0.05, $\Delta\mu_{Mo,0}$= 20 kJ/mol, and $\overline{V}_{gb,Mo} = 0.7\overline{V}_{g,Mo}$ for T= 500, 800, 1100, and 1400 K in (a2), (b2); $\Delta\mu_{Mo,0}$= 20 kJ/mol, T=800 K, and X= 0.05 for $\overline{V}_{gb,Mo}$= 0.9, 0.7, and 0.5 $\overline{V}_{g,Mo}$ in (a3), (b3); and $\Delta\mu_{Mo,0}$= 20 kJ/mol, T=800 K, and $\overline{V}_{gb,Mo} = 0.7\overline{V}_{g,Mo}$ for X= 0.005, 0.01, 0.02, 0.05, 0.1, and 0.2 in (a4), (b4). The horizontal dashed lines in (b2)-(b4) show the original GB free energy density γ^0=1 J/m^2 and the horizontal dashed line in (b1) indicates γ=0.

Figure 6(a1)-(a4). The values of γ are negative when the grain sizes are larger than $21L_0/\Omega_0$ and $14L_0/\Omega_0$ for $\Delta\mu_{Mo,0}$= 40 and 80 kJ/mol, respectively, as indicated in Figure 6(b1), whereas all values of γ are positive in the entire range of

grain size for $\Delta\mu_{\mathrm{Mo},0}$= 0, 5, 10, and 20 kJ/mol. The result is consistent with that of excess concentration Γ_{Mo} shown in Figure 6(a1), where the values of $c_{\mathrm{Mo}}^{\mathrm{gb,ex}}$ for $\Delta\mu_{\mathrm{Mo},0}$= 40 and 80 kJ/mol are much higher than the others. Comparing Figure 6(b1) with Figure 5(a1) illustrates an interesting phenomena that when the grain size is sufficiently large, the difference in molar free energy approaches zero regardless of the value of $\Delta\mu_{\mathrm{Mo},0}$, while the excess GB free energy per unit GB area for $\Delta\mu_{\mathrm{Mo},0}$= 80 kJ/mol approaches the most negative value of −10.6469 J/m^2, implying the inconsistence between the two properties. This inconsistence is attributed to the intrinsically distinct natures that the difference in molar free energy represents the difference in whole free energy between a NG polycrystalline alloy and its reference single crystal with the same nominal chemical composition and at the same temperature, whereas the variation in excess GB free energy, in contrast, signifies the excess free energy merely in the GB volume. The thermodynamic justification strongly suggests that the difference in molar free energy of NG polycrystalline alloy with respect to the reference of single crystal should be used in the study of thermal stability of the NG alloy. Based on this thermodynamic justification, the criterion for thermal stability is defined by the difference in molar free energy. A positive or negative difference in molar free energy of a NG alloy indicates the NG alloy is unstable or stable against the reference single crystal with the same nominal solute concentration at the same temperature. A zero value of difference in molar free energy of a NG alloy gives the critical grain size, at which a polycrystalline NG alloy possesses the same free energy as its reference single crystal. With this criterion, Figure 5(a2)-(a4) show the thermal stable regions of grain size for various temperatures, several partial molar volumes, and a number of nominal solute concentrations, although Figure 6(b2)-(b4) illustrate that for the same input parameters, the values of excess GB free energy per unit GB area are all positive.

In brief, Figure 6(a1)-(a4) and (b1)-(b4) illustrate that GB segregation and relaxation yield the excess solute concentration in GBs and reduce the GB excess free energy, and both are local properties only in the GB region.

4 Concluding remarks

The present work thermodynamically studies the multiple coupling effects of GB segregation and associated internal stresses on the thermal stability of NG alloys by utilizing the 3D interphase treatment of GBs. The stress-free single crystal with the same nominal chemical composition as that of a studied NG alloy is taken as reference in the theoretical analysis of GB segregation and relaxation. The theoretical study derives the analytic formulas about chemical compositions, strains, stresses, and free energies in both GBs and grains. GB segregation and relaxation is a natural internal process in NG alloys towards thermodynamic equilibrium, which occurs unavoidably in the NG alloys at a given temperature without any applied mechanical loads and constraints. The present thermodynamic analysis leads to the generalized capillary equation, the traction continuity boundary condition along the normal direction of GBs, and the chemical equilibrium condition, and thus develops further the thermodynamic foundation for the study of thermal stability of NG alloys, especially in the multiple coupling analysis between GB segregation and stresses. The 3D interphase treatment of GBs introduces some new properties of GBs, which should be determined by atomistic calculations or/and by meticulous experiments. The present thermodynamic analysis is carried out for alloys of multiple elements in solid solution, while the binary regular solid solution of $\mathrm{Ni}_{1-X}\mathrm{Mo}_X$ alloys is taken herein as an example to illustrate the results from the theoretical analysis. To demonstrate the important role of $\Delta\mu_{\mathrm{Mo},0}$, viz. the standard Gibbs free energy of segregation, various values of $\Delta\mu_{\mathrm{Mo},0}$ are taken in the figure demonstrations, although for a given NG alloy, the statistic mean of $\Delta\mu_{\mathrm{Mo},0}$ has a certain value. In summary, concluding remarks are highlighted below from the present thermodynamic study of the thermal stability of NG alloys.

(1) GB segregation is caused by solute atoms moving from grains to GBs and hence yields the differentiation of the chemical composition induced eigenstrains, which is further converted to the chemical GB eigenstress in the hybrid analysis of eigenstrain and eigenstress. The relaxation process releases the GB total eigenstress, causes deformation, and generates stress in grains, meanwhile reducing the total energy of NG alloys. The internal stresses in NG alloys after GB segregation and relaxation can be extremely high, reaching the GPa level.

(2) The internal stresses induced by GB segregation and relaxation play an important role in the thermal stability of NG alloys, especially via the coupling terms between stress and concentration. The magnitude of the difference in molar free energy will be greatly underestimated without counting the stress-involved terms in the thermodynamic analysis.

(3) The difference in molar free energy, rather than the GB excess free energy per unit area, should be the right criterion of thermal stability of NG alloys. The difference in molar free energy represents the difference in whole free energy between a NG polycrystalline alloy and its reference single crystal with the same nominal chemical composition and at the same temperature, while the excess GB free energy, in contrast, signifies merely the excess free energy between the GB and grain regions.

(4) The thermal stability of a NG alloy is determined by the

difference in molar free energy. A positive or negative difference in molar free energy indicates the NG alloy is unstable or stable against the reference single crystal, which is controlled by the grain size, nominal chemical composition, temperature, and other thermodynamic properties of GBs and grains.

This work was supported by the National Key R&D Program of China (Grant No. 2017YFB0701604). Sheng Sun also acknowledge the National Natural Science Foundation of China (Grant No. 11672168) for financial support.

1 E. O. Hall, Proc. Phys. Soc. Sect. B **64**, 747 (1951).
2 N. J. Petch, J. Iron Steel Instit. **174, 25** (1953).
3 C. C. Yang, and Y. W. Mai, Mater. Sci. Eng.-R-Rep. **79**, 1 (2014).
4 G. Wang, J. Lian, Q. Jiang, S. Sun, and T. Y. Zhang, J. Appl. Phys. **116**, 103518 (2014).
5 R. I. Babicheva, D. V. Bachurin, S. V. Dmitriev, Y. Zhang, S. W. Kok, L. Bai, and K. Zhou, Philos. Mag. **96**, 1598 (2016).
6 Y. Z. Zhang, J. B. Liu, and H. T. Wang, Sci. China Tech. Sci. **62**, 546 (2019).
7 K. Lu, Nat Rev Mater **1**, 16019 (2016).
8 T. Chookajorn, H. A. Murdoch, and C. A. Schuh, Science **337**, 951 (2012).
9 J. Hu, Y. N. Shi, X. Sauvage, G. Sha, and K. Lu, Science **355**, 1292 (2017).
10 J. Hui, W. Liu, and B. Wang, Sci. China-Phys. Mech. Astron. **63**, 104612 (2020).
11 X. Zhou, X. Y. Li, and K. Lu, Science **360**, 526 (2018).
12 X. Zhou, X. Li, and K. Lu, Phys. Rev. Lett. **122**, 126101 (2019).
13 J. Weissmüller, Nanostruct. Mater. **3**, 261 (1993).
14 W. C. Johnson, and J. M. Blakely, *Surface Segregation in Metals and Alloys* (ASM, Metals Park, 1979), pp. 3-23.
15 H. J. Fecht, Phys. Rev. Lett. **65**, 610 (1990).
16 J. F. Rico, R. López, and J. I. F. Alonso, Phys. Rev. A **29**, 6 (1984).
17 X. Zhang, S. Sun, T. Xu, and T. Y. Zhang, Sci. China Tech. Sci. **62**, 1565 (2019).
18 A. R. Kalidindi, T. Chookajorn, and C. A. Schuh, JOM **67**, 2834 (2015).
19 A. R. Kalidindi, and C. A. Schuh, Acta Mater. **132**, 128 (2017).
20 F. Abdeljawad, P. Lu, N. Argibay, B. G. Clark, B. L. Boyce, and S. M. Foiles, Acta Mater. **126**, 528 (2017).
21 R. Dingreville, and S. Berbenni, Acta Mater. **104**, 237 (2016).
22 T. Y. Zhang, and J. E. Hack, Phys. Stat. Sol. (a) **131**, 437 (1992).
23 P. Lejček, and S. Hofmann, Acta Mater. **170**, 253 (2019).
24 H. R. Peng, M. M. Gong, Y. Z. Chen, and F. Liu, Int. Mater. Rev. **62**, 303 (2017).
25 M. Saber, C. C. Koch, and R. O. Scattergood, Mater. Res. Lett. **3**, 65 (2015).
26 J. Weissmüller, J. Mater. Res. **9**, 4 (1994).
27 R. Kirchheim, Acta Mater. **50**, 413 (2002).
28 F. Liu, and R. Kirchheim, Scripta Mater. **51**, 521 (2004).
29 F. Liu, and R. Kirchheim, J. Cryst. Growth **264**, 385 (2004).
30 K. A. Darling, M. A. Tschopp, B. K. VanLeeuwen, M. A. Atwater, and Z. K. Liu, Comput. Mater. Sci. **84**, 255 (2014).
31 J. R. Trelewicz, and C. A. Schuh, Phys. Rev. B **79**, 9 (2009).
32 M. Saber, H. Kotan, C. C. Koch, and R. O. Scattergood, J. Appl. Phys. **113**, 063515 (2013).
33 M. Saber, H. Kotan, C. C. Koch, and R. O. Scattergood, J. Appl. Phys. **114**, 103510 (2013).
34 P. Wynblatt, and R. C. Ku, Surf. Sci. **65**, 511 (1977).
35 J. Friedel, Adv. Phys. **3**, 446 (1954).
36 F. Tang, X. Liu, H. Wang, C. Hou, H. Lu, Z. Nie, and X. Song, Nanoscale **11**, 1813 (2019).
37 T. Krauß, and S. M. Eich, Acta Mater. **187**, 73 (2020).
38 T. Y. Zhang, H. Ren, Z. J. Wang, and S. Sun, Acta Mater. **59**, 4437 (2011).
39 P. W. Voorhees, and W. C. Johnson, Solid State Phys.-Adv. Res. Appl. **59**, 1 (2004).
40 T. Y. Zhang, and H. Ren, Acta Mater. **61**, 477 (2013).
41 J. Weissmüller, and J. W. Cahn, Acta Mater. **45**, 1899 (1997).
42 T. Y. Zhang, M. Luo, and W. K. Chan, J. Appl. Phys. **103**, 104308 (2008).
43 J. Weissmüller, H. L. Duan, and D. Farkas, Acta Mater. **58**, 1 (2010).
44 J. W. Gibbs, *The Scientific Papers* (Dover Publications, New York, 1961), pp. 55-354.
45 D. McLean, *Grain Boundaries in Metals* (Oxford University Press, London, 1957).
46 T. Mura, *Micromechanics of Defects in Solids*, 2nd ed (Martinus Nijhoff Publishers, Dordrecht, 1987).
47 H. Ren, X. Yang, Y. Gao, and T. Y. Zhang, Acta Mater. **61**, 5487 (2013).
48 C. Lemier, and J. Weissmüller, Acta Mater. **55**, 1241 (2007).
49 T. Mütschele, and R. Kirchheim, Scripta Metall. **21**, 135 (1987).
50 H. Ren, and T. Y. Zhang, Mater. Lett. **130**, 176 (2014).
51 H. Cai, J. W. Mai, Y. X. Gao, H. Huang, S. Sun, and T. Y. Zhang, Sci. China Tech. Sci. **62**, 1735 (2019).
52 Z. K. Liu, B. Li, and H. Lin, J. Phase Equilib. Diffus. **40**, 508 (2019).
53 J. W. Cahn, Acta Metall. **9**, 795 (1961).
54 J. Zhu, Y. Gao, D. Wang, J. Li, T. Y. Zhang, and Y. Wang, Mater. Horiz. **6**, 515 (2019).
55 T. Y. Zhang, Z. J. Wang, and W. K. Chan, Phys. Rev. B **81**, 195427 (2010).
56 A. Pathak, K. K. Mehta, and A. K. Singh, J. Appl. Res. Tech. **15**, 78 (2017).
57 A. T. Dinsdale, Calphad **15**, 317 (1991).
58 H. Gleiter, Prog. Mater. Sci. **33**, 223 (1989).
59 C. Suryanarayana, Int. Mater. Rev. **40**, 41 (1995).
60 J. Weissmuller, and C. Lemier, Philos. Mag. Lett. **80**, 411 (2000).
61 X. Y. Zhou, B. L. Huang, and T. Y. Zhang, Phys. Chem. Chem. Phys. **18**, 21508 (2016).
62 X. Y. Zhou, H. Ren, B. L. Huang, and T. Y. Zhang, Sci. China Tech. Sci. **57**, 680 (2014).